The Geological Society of America
Special Paper 555

The lithospheric folding model applied to the Bighorn uplift during the Laramide orogeny

B. Tikoff*
Department of Geoscience, University of Wisconsin–Madison, 1215 W. Dayton Street, Madison, Wisconsin 53706, USA

C. Siddoway
Department of Geology, Colorado College, Colorado Springs, Colorado 80903, USA

D. Sokoutis
Department of Earth Sciences, Utrecht University, Princetonlaan 4, 3584 CB Utrecht, Netherlands, and
Department of Geosciences, University of Oslo, P.O. Box 1047, Blindern, N-0316 Oslo, Norway

E. Willingshofer
Department of Earth Sciences, Utrecht University, Princetonlaan 4, 3584 CB Utrecht, Netherlands

ABSTRACT

The Bighorn uplift, Wyoming, developed in the Rocky Mountain foreland during the 75–55 Ma Laramide orogeny. It is one of many crystalline-cored uplifts that resulted from low-amplitude, large-wavelength folding of Phanerozoic strata and the basement nonconformity (Great Unconformity) across Wyoming and eastward into the High Plains region, where arch-like structures exist in the subsurface. Results of broadband and passive-active seismic studies by the Bighorn EarthScope project illuminated the deeper crustal structure. The seismic data show that there is substantial Moho relief beneath the surface exposure of the basement arch, with a greater Moho depth west of the Bighorn uplift and shallower Moho depth east of the uplift. A comparable amount of Moho relief is observed for the Wind River uplift, west of the Bighorn range, from a Consortium for Continental Reflection Profiling (COCORP) profile and teleseismic receiver function analysis of EarthScope Transportable Array seismic data.

The amplitude and spacing of crystalline-cored uplifts, together with geological and geophysical data, are here examined within the framework of a lithospheric folding model. Lithospheric folding is the concept of low-amplitude, large-wavelength (150–600 km) folds affecting the entire lithosphere; these folds develop in response to an end load that induces a buckling instability. The buckling instability focuses initial fold development, with faults developing subsequently as shortening progresses. Scaled physical models and numerical models that undergo layer-parallel shortening

*E-mail: basil@geology.wisc.edu

Tikoff, B., Siddoway, C., Sokoutis, D., and Willingshofer, E., 2022, The lithospheric folding model applied to the Bighorn uplift during the Laramide orogeny, *in* Craddock, J.P., Malone, D.H., Foreman, B.Z., and Konstantinou, A., eds., Tectonic Evolution of the Sevier-Laramide Hinterland, Thrust Belt, and Foreland, and Postorogenic Slab Rollback (180–20 Ma): Geological Society of America Special Paper 555, https://doi.org/10.1130/2021.2555(08).

induced by end loads determine that the wavelength of major uplifts in the upper crust occurs at approximately one third the wavelength of folds in the upper mantle for strong lithospheres. This distinction arises because surface uplifts occur where there is distinct curvature upon the Moho, and the vergence of surface uplifts can be synthetic or antithetic to the Moho curvature. In the case of the Bighorn uplift, the surface uplift is antithetic to the Moho curvature, which is likely a consequence of structural inheritance and the influence of a preexisting Proterozoic suture upon the surface uplift. The lithospheric folding model accommodates most of the geological observations and geophysical data for the Bighorn uplift. An alternative model, involving a crustal detachment at the orogen scale, is inconsistent with the absence of subhorizontal seismic reflectors that would arise from a throughgoing, low-angle detachment fault and other regional constraints. We conclude that the Bighorn uplift—and possibly other Laramide arch-like structures—is best understood as a product of lithospheric folding associated with a horizontal end load imposed upon the continental margin to the west.

INTRODUCTION

The mode of formation of the Laramide-style block uplifts, at a significant distance from the western plate margin of Laurentia, is a long-standing problem in North American geology. Cored by crystalline basement, these uplifts occur east of the Sevier fold-and-thrust belt, in a belt that crosses Montana, Wyoming, South Dakota, Utah, Colorado, Arizona, and New Mexico (e.g., Oldow et al., 1989; Burchfiel et al., 1992; Snoke, 1993). The structures also are found in the subsurface beneath the High Plains, where they are sometimes continuous with exposed uplifts (e.g., the subsurface Chadron arch of Nebraska connects with the exposed Black Hills uplift of South Dakota) but are buried by Tertiary strata (e.g., Merriam, 1963; Tikoff and Maxson, 2001). As highlighted by Erslev (1993) and others, the structures form broad, arch-like, regional-scale folds of Phanerozoic strata and the underlying Great Unconformity. Some are associated with positive gravity anomalies, as is the case for the Bighorn Mountains (Kucks and Hill, 2000; Worthington et al., 2016).

The timing of the uplifts is well recorded by sedimentological relations in immediately adjacent basins, which indicate a Late Cretaceous–Paleogene age (e.g., Dickinson et al., 1988). Thermochronology data from the block uplifts in Montana have recently documented the initiation of uplift at ca. 100 Ma (Carrapa et al., 2019), consistent with earlier interpretations of pre-Paleogene uplift in specific ranges (e.g., Wind River Range; Steidtmann and Middleton, 1991). Because steeply dipping faults exposed at Earth's surface flank the block uplifts and are associated with steep attitudes of bedding in cover strata, early workers considered the possibility that the basement-cored uplifts resulted from vertical tectonics (Palmquist, 1978; Stearns, 1978). On the basis of the seismic results of the Wind River Range in Wyoming obtained by Smithson et al. (1978, 1979) and subsequent geophysical surveys, it is now well accepted that the Laramide-style block uplifts resulted from horizontal contraction (e.g., Weil and Yonkee, 2012; Weil et al., 2014).

Four differing models for formation for thick-skinned deformation and the development of the basement-uplift structures were summarized by Erslev (2005) and Yeck et al. (2014). These are: (1) pure shear lithospheric shortening and thickening (Kulik and Schmidt, 1988; Egan and Urquhart, 1993), (2) domino-style fault blocks at lithospheric scale (McQueen and Beaumont, 1989); (3) crustal detachment (Erslev, 1993; Worthington et al., 2016); and (4) lithospheric buckling (Tikoff and Maxson, 2001). Proposed tectonic mechanisms include end loading at plate margins (Maxson and Tikoff, 1996; Tikoff and Maxson, 2001; Saleeby 2003), weakening from below due to hydration by volatiles released from a subducted slab (Humphreys et al., 2003), and others that arise from structural inheritance or subcrustal shear (Bird, 1988).

The EarthScope Bighorn Project focused on the Bighorn uplift of northern Wyoming as an opportune site at which to test the four competing models for Laramide uplifts. The project involved both active-source and passive-source acquisition of seismic data, and collection of gravity data and structural geology measurements, to image the lithospheric structure below the Bighorn Mountains and obtain three-dimensional (3-D) geometry of the basement-cored Bighorn uplift and neighboring basins (Fig. 1). Each of the four competing models make predictions about the geometry of the crust, mantle, and Moho (crust-mantle boundary) at a scale that would be distinguishable in the regional 3-D data sets (Fig. 2). In the case of pure shear thickening (1), a downward deflection of the Moho would be observed beneath the crest of the basement uplift, together with a negative gravity anomaly (Fig. 2A). Further, for this model, a relation should exist between Moho offset and linear, asymmetric gravity anomalies. In the case of domino-style faulting of the entire lithosphere (2), clear offsets of the Moho and lithospheric layering would be evident, at a regular spacing (Fig. 2A). These first two models have been ruled out, on the basis of the variable but smooth Moho geometry determined from the Bighorn Arch Seismic Experiment (BASE), using both active-source P-wave velocity

structure (Worthington et al., 2016) and passive-source teleseismic receiver function analysis (Yeck et al., 2014), as well as gravity analysis (Worthington et al., 2016). In the case of a crustal detachment (3), as postulated by the Bighorn Project, the Moho should be imaged as flat, and a gravity anomaly is not expected (Fig. 2A). Lithospheric folding (buckling) (4), as postulated by the Bighorn Project, should result in an upward deflection of the Moho beneath the Bighorn uplift and a positive gravity anomaly due to the upwarp of mantle (not shown on Fig. 2A). The geometry of the Moho determined from the Bighorn Project seismic results (Fig. 2) suggests that the latter two models are permissible and merit consideration.

In this study, we utilized the results of the Bighorn Project to examine lithospheric folding as a viable mechanism and causative model for the Bighorn uplift. First, we reviewed the results of the seismic data from the region below the Bighorn uplift and adjacent basins, and the occurrence of the Bighorn uplift at an inflection point in a curved Moho geometry. We also summarized some pertinent paleomagnetic data from the Bighorn region (Weil et al., 2014). Second, we reviewed recent analog modeling and numerical models of lithospheric folding and compared these models to the geometry of the Moho below the Bighorn uplift and periodicity of crustal uplifts. We synthesized the seismic data with the results of the analog models to show a remarkable coherence between the two data sets, which matches the predictions of the lithospheric folding model. Further, we addressed the role of a preexisting shear zone that could have caused the observed arch asymmetry and eastward vergence of the Bighorn uplift

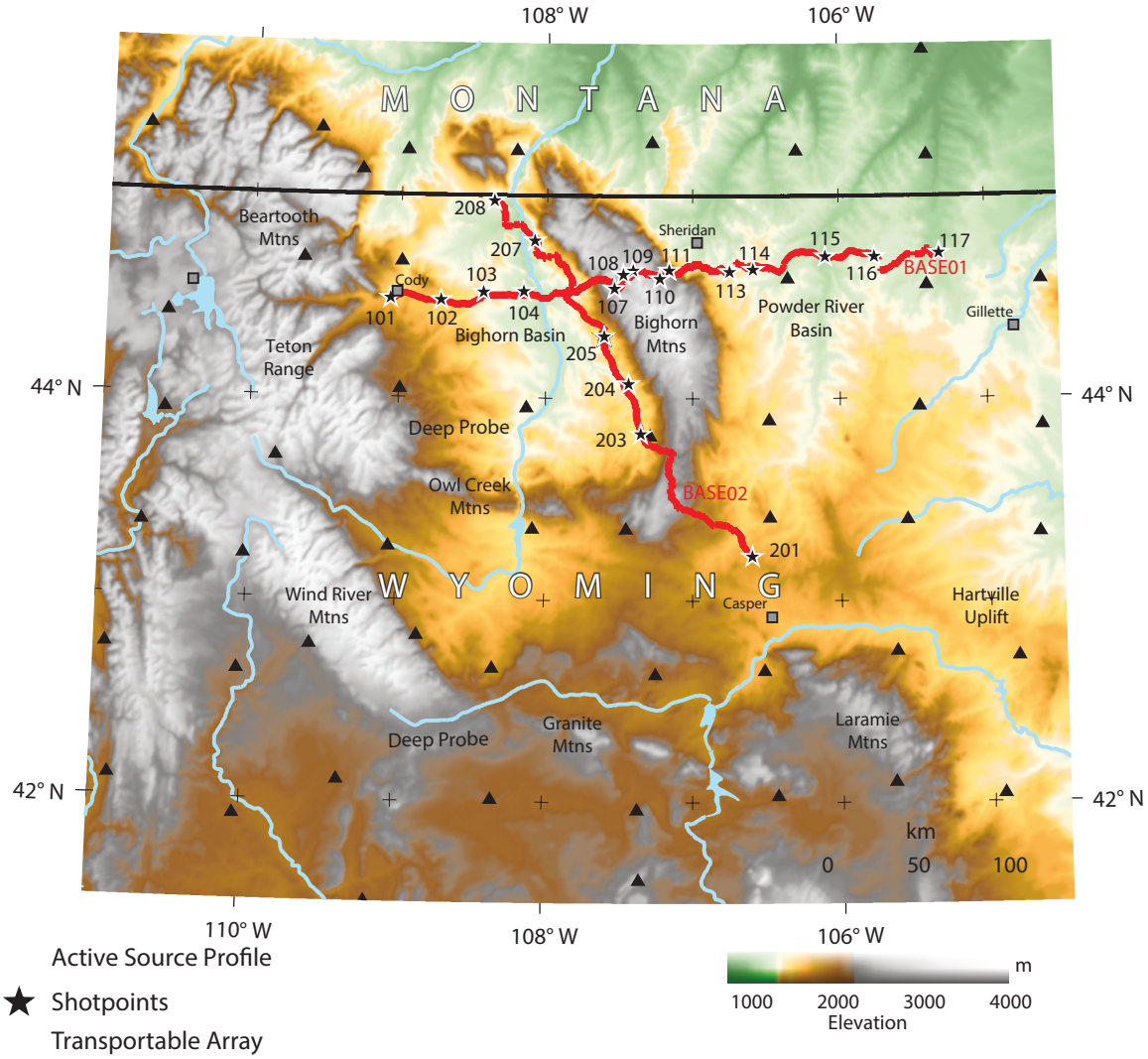

Figure 1. Topographic map of Wyoming and southern Montana, modified from Worthington et al. (2016), with all block uplifts (black) labeled. Basins proximal to the Bighorn uplift are also labeled. Red lines show locations of the active source geophones of Worthington et al. (2016). Closely spaced broadband seismometers of the Yeck et al. (2014) study follow the same E-W line as Worthington et al. (2016). Filled black triangles are stations from the EarthScope transportable array.

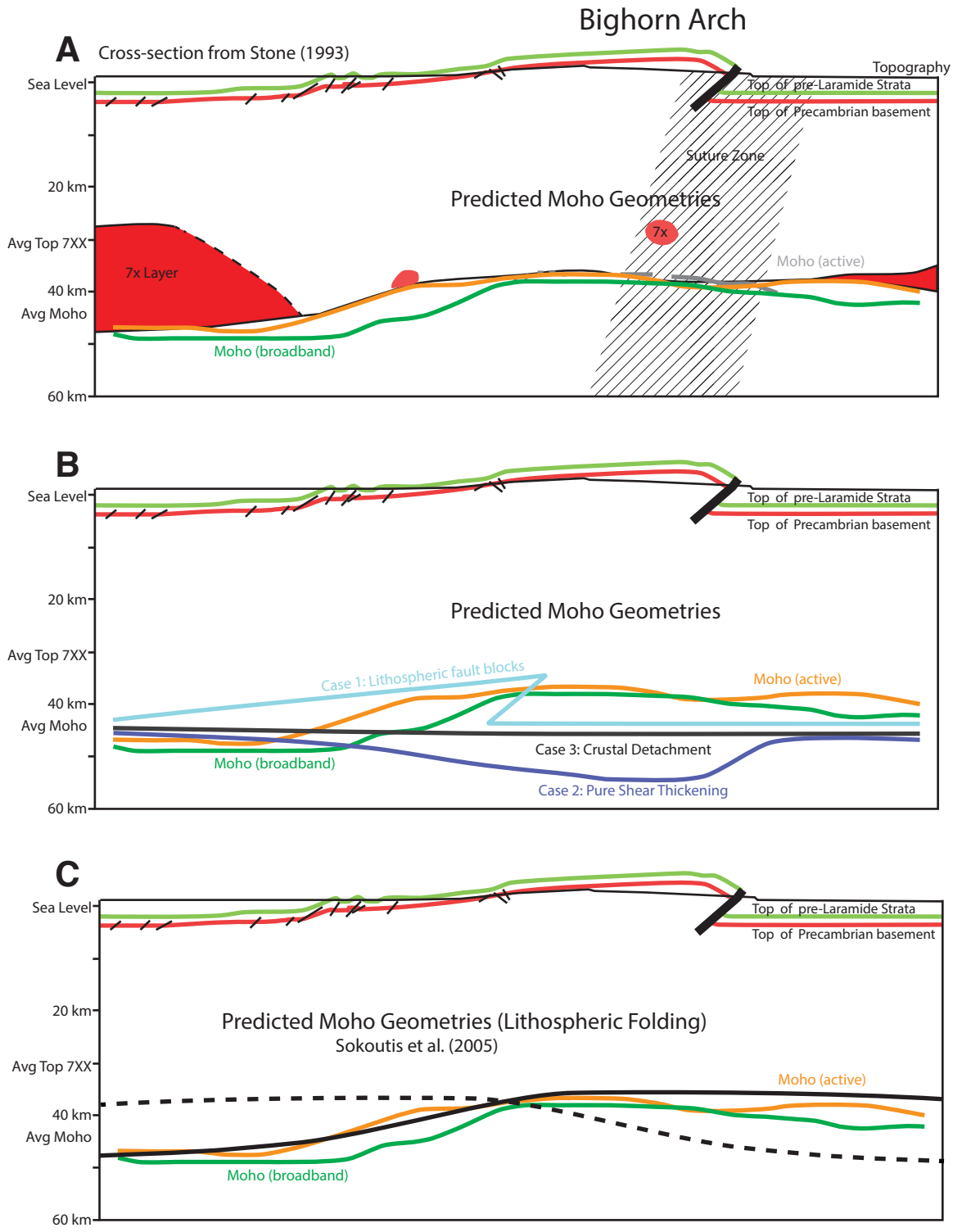

Figure 2. Lithospheric cross sections through the Bighorn uplift. The upper-crustal geometry, and particularly the use of the Tensleep Formation as a marker, relies on the work of Stone (1993). (A) Interpretations of seismic data from the Bighorn Project. The Moho geometry from receiver functions from broadband seismometers is shown in green (Yeck et al., 2014) and orange (Worthington et al., 2016). The Moho geometry (orange line) and presence of 7.x layers (red areas) on both sides, but not underneath, of the Bighorn uplift are from the active seismic results of Worthington et al. (2016). The interpretation of a W-dipping Proterozoic suture zone is also shown. (B) Three proposed Moho geometries for the Bighorn uplift, based on different lithospheric deformation models for uplift in the Rocky Mountains (from Yeck et al., 2014). These models are: (1) lithospheric fault blocks, (2) lower-crustal pure shear thickening, and (3) crustal detachment. These schematic models are superimposed on the actual geometry determined by Yeck et al. (2014; green line) and Worthington et al. (2016; orange line). (C) Two possible schematic (solid and dashed lines) Moho geometries based on the scaled models of Sokoutis et al. (2005). Because the crustal uplift can indicate either sense of vergence, relative to an inflection point in mantle folding, both options are equally permissible in the absence of other evidence.

(Stone, 2003). Finally, we argue that a crustal detachment model, as conceptualized in the orogenic float model (e.g., Oldow et al., 1989; Erslev, 2005), is not consistent with existing geophysical data and regional geological constraints. We conclude that the Bighorn uplift, as the type example of Laramide arch-like structures, likely formed as a result of lithospheric folding associated with a horizontal end load on the western continental margin of Laurentia in the Cretaceous–Paleogene.

GEOLOGICAL BACKGROUND: THE BIGHORN UPLIFT

The Bighorn Mountains are situated within Archean cratonic lithosphere of the Wyoming Province. Crystalline rocks forming the core of the Bighorn Mountains arch consist of the 2.84 Ga Bighorn Batholith and preexisting gneisses (Frost and Fanning, 2006; Mueller and Frost, 2006). Granitoids of the Bighorn Batholith show domainal fabric development, including the presence of several crosscutting mylonite belts (Malone et al., 2019). Low-temperature thermochronology data show that crystalline rocks in the Bighorn uplift attained a position in the shallow crust during two Proterozoic cooling episodes (1800–1600 Ma and 900–525 Ma), and at no point since 960 Ma did temperatures exceed 220 °C (Reiners and Farley, 2001; Orme et al., 2016). This history suggests a prolonged period of tectonic stability following the amalgamation of Proterozoic tectonic provinces to the craton south of the Cheyenne belt and east of the Trans-Hudson belt (Whitmeyer and Karlstrom, 2007).

Phanerozoic sedimentary formations in northern Wyoming are up to 4 km thick (e.g., Beaudoin et al., 2014). In the Phanerozoic section, zircon helium data detect a cooling episode between 85 and 60 Ma, when rocks beneath the Great Unconformity cooled from ~115 °C to 50 °C during Sevier-Laramide tectonism (Orme et al., 2016). Under conditions of a representative continental geotherm, the cooling could have been achieved by stripping of sedimentary cover and exhumation of bedrock from a depth of ~4 km to ~1.5 km, without appreciable erosion into the crystalline basement rock. Prominent topographic lineaments that trend E-W to NE-SW across the Bighorn Range display only small displacement of Mesozoic and older strata, up to 200 m (Doane, 2010), insufficient to affect the thermal structure of basement.

Thick-skinned deformation and basement-involved uplifts are signature features of the Laramide orogeny in the Rocky Mountains of the United States (Stearns, 1978; Yonkee and Weil, 2015) that provide a model for recognition of foreland deformation elsewhere. Intermontane basins separate the basement uplifts. The structural relief between basin and uplift may exceed 8 km, but the overall strain is low (~10% shortening; e.g., Brown, 1993; Stone, 1993). Arch geometries may be symmetrical or asymmetrical (cf. Stanton and Erslev, 2004; Sharry et al., 1986, COCORP).

Weil et al. (2014) presented results from the Bighorn arch, in which they utilized rock magnetic properties to evaluate the direction of layer-parallel shortening (using anisotropy of magnetic susceptibility [AMS]) and rotation (using paleomagnetism). This same approach was used in evaluating deformation associated with the Utah-Idaho-Wyoming segment of the Sevier thrust belt (e.g., Yonkee and Weil, 2010; Weil and Yonkee, 2012), to which they compared their results. Figure 3 shows the result of their paleomagnetic results, which were conducted solely on the Triassic Chugwater Formation, because the presence of hematite provided a strong magnetic remanence carrier. The critical result is that most sites, within error, point northerly, in the polarization direction acquired under influence of the Triassic reference pole. Thus, the Triassic and younger units have not undergone statistically significant vertical axis rotation; only very minor counterclockwise rotation could have occurred in the NE part of their study area. The AMS results of Weil et al. (2014), combined with kinematic results for minor fault populations, indicate a ENE-WSW–trending direction of layer-parallel shortening on both sides of the Bighorns, although the directions are more NE-SW trending on the west side. Adjacent to the Tensleep fault (Fig. 3), there seems to be rotation of the layer-parallel shortening direction that may be attributable to wrench displacement upon the Tensleep fault. Except for this localized difference, the analyses overall indicate that Triassic and younger strata have not undergone vertical axis rotation. In contrast, correlative formations involved in deformation along the margins of the Sevier thrust belt did undergo vertical axis rotation (e.g., Weil and Yonkee, 2012). Weil et al. (2014) attributed the difference to the effects of two distinct mechanical systems: (1) a Sevier fold-and-thrust belt that is deformed by stresses active above a weak basal detachment; and (2) Laramide-style uplifts, which occurred in response to stresses transferred through the deeper crust or mantle lithosphere.

Results of EarthScope Bighorn Project

The major results of the Bighorn Project were presented by Yeck et al. (2014) and Worthington et al. (2016). Below, we summarize the results of this work in order to constrain different models for the Laramide-age uplift of the Bighorn Mountains. A tectonic model for the Bighorn uplift must account for several geological and geophysical results from the EarthScope broadband and passive-active seismic study, and the broader context provided by USArray and legacy data sets (Fig. 2B). Key observations are: (1) The Moho is higher (~37 km below the surface) east of the Bighorn uplift than it is west of the uplift (~50 km below the surface); (2) the Moho is "bulged" up ~3 km below portions of the surface exposure of the basement arch; (3) a high-velocity, high-density material (the "7.x layer") is absent in the lower crust beneath the arch culmination; and (4) there is a lack of subhorizontal reflectors that could be associated with a regional detachment. In addition, there are two interpretations that should be considered: (1) Crustal thicknesses likely varied prior to the Laramide-age deformation; and (2) the Bighorn uplift borders a NNW-trending geophysical anomaly inferred to be an E-dipping Proterozoic suture.

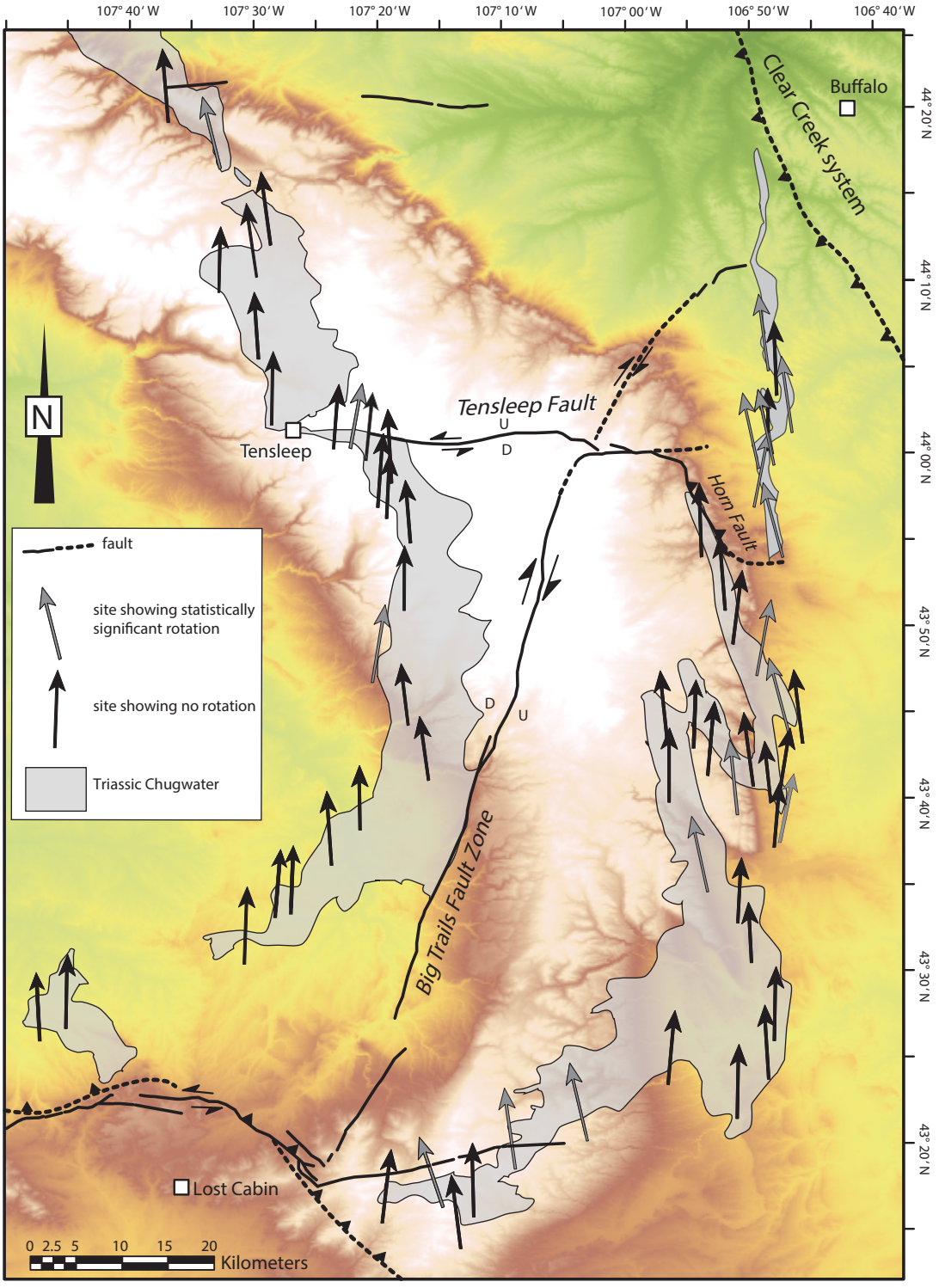

Figure 3. Paleomagnetic results from the Triassic Chugwater Formation surrounding the Bighorn uplift, with rotation shown with respect to the reference pole for cratonic North America, simplified from Weil et al. (2014). Black arrows show no statistically significant rotation, which characterizes the majority of the field area. Gray arrows show minor, but statistically significant, rotation; the only pattern is very minor counterclockwise rotation in the NE portion of the field area.

LITHOSPHERIC FOLDING: A REVIEW

Background

Because the concept of lithospheric folding is not well known in the North American geology community, we here provide a synopsis of this concept. This description includes how this idea was originally applied to the Laramide-style uplifts in the Rocky Mountains and High Plains region of the western United States. Interested readers may choose more thorough reviews of this subject by Ziegler et al. (1998), Cloetingh et al. (1999), and Cloetingh and Burov (2011).

Folding of layered sequences, at a periodic or semi-periodic wavelength, is a well-known feature in structural geology. The folding instability results as a dynamic of a thin plate subjected to an end load. The mechanics of this formation was theoretically developed by Biot and others (Biot, 1965; Ramberg, 1981). Scaled analog materials that demonstrated this behavior are particularly exemplified by the work of Ramberg and collaborators (e.g., Ramberg, 1963, 1981). This theory was applied successfully to rocks in the field (e.g., Hudleston, 1973). These workers showed that a layer would initiate a fold—a process known as buckling—at a periodic wavelength controlled by the strength of the folded unit. In areas with multiple layered units, the folding could occur at the wavelength of the strongest layer, in which a secondary strong layer could produce a second-order folding pattern that was superimposed on the overall wavelength. This combination of multiple strong layers results in a periodic wavelength with superimposed minor, second-order folds ("s," "z," "m," or "w" folds), which are commonly observed in field settings. In some cases, the wavelength is thought to reflect the combination of the strength of all layered rocks within a sequence.

The concept that the entire lithosphere could also respond to an end load, as could occur during continental collision, was introduced as "lithospheric buckling" (Fig. 4A). This term was superseded by the term "lithospheric folding" in the 2000s, probably because the buckling mechanism refers only to the initiation of the folding process. The idea was introduced into the geological literature in the late 1980s and early 1990s, primarily by French researchers conducting analog (sand and silicon) experiments (e.g., Faugere and Brun, 1984; Davy and Cobbold, 1988, 1991; Martinod, 1991; Martinod and Davy, 1992). The scaling in these models was based on the experimentally determined flow laws being produced for experimental rock deformation of monophase rocks (e.g., quartz, plagioclase, olivine) and then applied to specific lithospheric layers (e.g., Brace and Kohlstedt, 1980; Kirby, 1983, 1985; Ranalli and Murphy, 1987). The applicability of the analog modeling was strongly supported by seismic studies of the Indian plate immediately south of continental India, in which the periodic folding of the Moho is observed at wavelengths similar to those predicted by the analog models (McAdoo and Sandwell, 1985).

The work was subsequently supported by a variety of numerical studies that showed similar buckling behavior of the lithosphere as a result of end loading. Based on numerical models by Burov et al. (1993), Cloetingh et al. (1999) characterized the wavelength of lithospheric folding based on the thermo-tectonic age of the lithosphere (Fig. 4B). The thermo-tectonic age of the lithosphere is thought to reflect the time since the latest major thermal event. The wavelength depends on whether the upper crust controlled the buckling (wavelengths of up to ~60 km), the lithospheric mantle controlled the buckling (wavelengths of up to ~450 km), or the entire lithosphere controlled the buckling (wavelengths of up to ~600 km) (Fig. 4A). The modelers based their work upon specific localities worldwide that exhibited lithospheric buckling where they could estimate thermo-tectonic age. Lithospheric folding has since been applied to major crustal uplifts far from the edge of cratonic margins (e.g., Himalayas—Burg et al., 1994; Smit et al., 2013; Central Australia—Kennett and Iaffaldano, 2012; Eastern Europe—Starostenko et al., 2013).

Application to the Rocky Mountains

Prior investigators used folding models and developed an application of a lithospheric folding model to understand the deformation of Wyoming and the Colorado Plateau region. Sales (1968) created a series of analog experiments that successfully reproduced many of the regional structures observed in Wyoming. These models were impactful and helped to resolve the "vertical tectonics" versus "horizontal tectonics" debates about uplifts in Wyoming, in favor of the latter. It appears, however, that it was the seismic studies of Smithson et al. (1978, 1979), which showed the thrust fault on the western edge of the Wind River Mountains gradually reducing its dip to a subhorizontal orientation, that fully resolved the issue in favor of horizontal tectonics.

Tikoff and Maxson (2001) applied the lithospheric buckling model to the Laramide orogeny. Their contribution pointed out that: (1) the wavelength of folding in the Rockies varies, but it is generally ~190 km and likely reflects mantle folding; (2) there are concealed folds in the High Plains that occurred in the Cretaceous–Paleogene on similar wavelengths to those observed in the Rocky Mountains, and sometimes continuous with an exposed uplift; and (3) the Laramide uplifts record a shortening direction in response to a mantle end load that differs from the orientation for thrust faults of the Sevier thrust belt, which are detached and driven by gravity (e.g., Weil and Yonkee, 2012). The lithospheric buckling model requires an end load on the western edge of North America, as opposed to a basal-traction mechanism as proposed by Bird (1988). In what becomes a critical point, Tikoff and Maxson (2001) assumed that the upper-crustal geometry would have some direct relation to the Moho geometry.

The lithospheric buckling model received formal and informal critiques prior to the EarthScope Bighorn Project. Erslev (2005) pointed out that the wavelength of the folding is variable, particularly with respect to the Rocky Mountains and the High Plains. Further, he estimated the Rocky Mountains and Colorado Plateau wavelengths to be more significantly closely spaced (e.g., 140 km for the Colorado Plateau compared to 190 km obtained

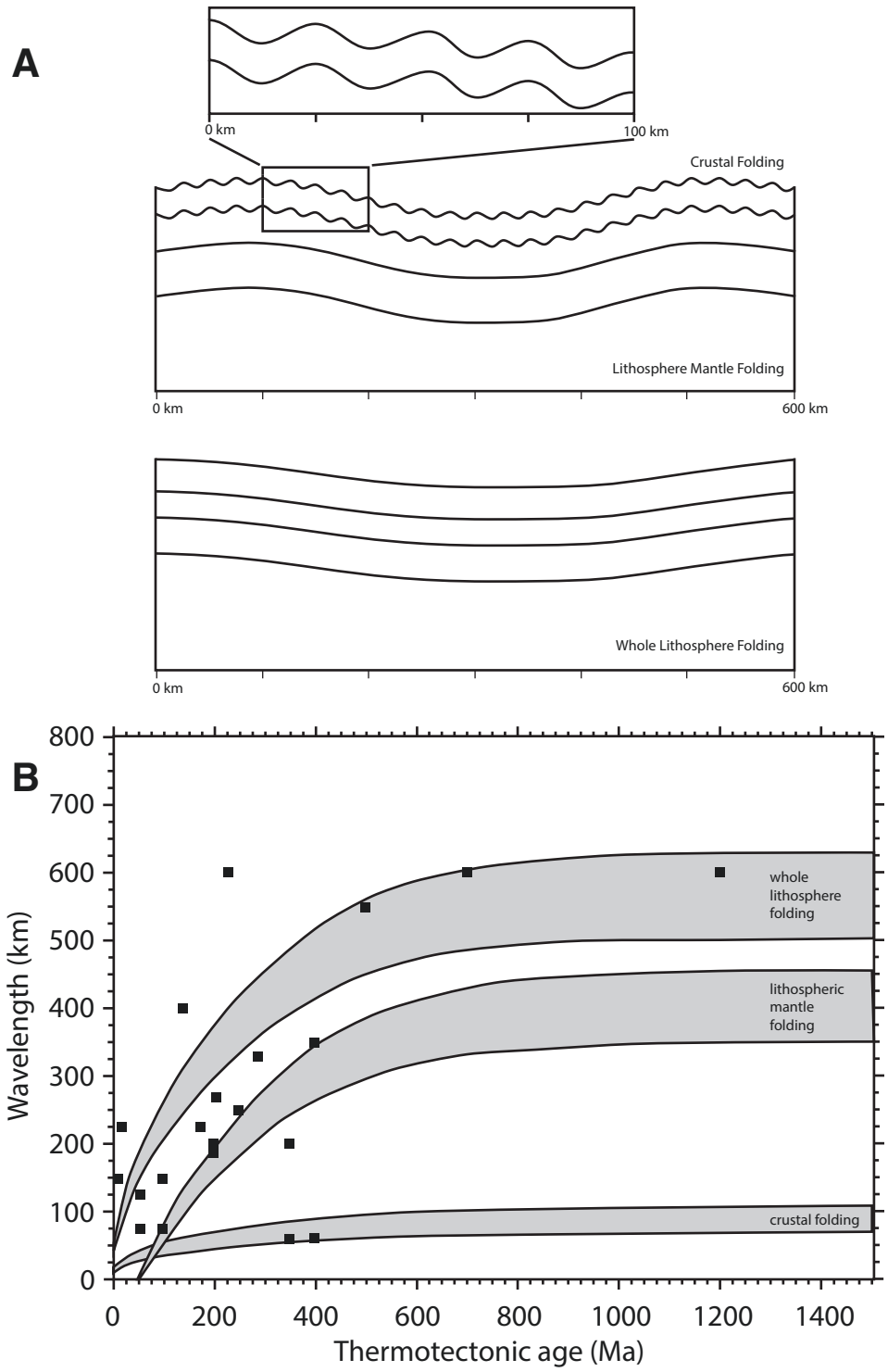

Figure 4. (A) Concept of lithospheric folding, with the three types of predicted folding and approximate wavelength: (1) upper-crustal folding (~20–40 km); (2) mantle lithosphere folding (~200–450 km); and (3) entire lithosphere folding (~300–600 km). (B) Lithospheric folding based on the thermo-tectonic age of the lithosphere, from Cloetingh et al. (1999). Note that upper-crustal folding can happen at the same time as mantle folding, similar to second-order (drag) folds observed on outcrop scale; upper-crustal folding cannot happen in whole lithosphere folding. Top cartoon emphasizes the duality of behavior for upper-crustal and mantle folding, but it gives the incorrect impression that more shortening occurs in the upper crust relative to lower parts of the lithosphere.

by Tikoff and Maxson, 2001). Partly at issue is whether the E-W–trending arches (Owl Creek, Granite, and Uinta Mountains) are included in the calculations (Erslev, 2005) or not (Tikoff and Maxson, 2001). Those uplifts likely formed late and with significant sinistral strike-slip movement during the formation of the Laramide uplifts. For the informal critique, S. Cloetingh (ca. 2004, personal commun. to B. Tikoff) noted that a longer wavelength was expected for mantle folding in the cold lithosphere of the Wyoming craton province of the Rocky Mountains. The age of the Wyoming craton, which was mostly unaffected by Paleozoic Ancestral Rockies deformation (e.g., Miller et al., 1992), is likely older than 1400 Ma. Using the calculations of Cloetingh

et al. (1999) (Fig. 4B herein), the wavelength of mantle folding should be ~400 km or more for strong, cold lithosphere. This issue is resolved below.

Subsequent Experimental Work

Scaled, analog experiments of lithospheric deformation applied to orogenic processes have advanced over the past two decades (Burg et al., 2002; Schellart, 2002; Pastor-Galán et al., 2012). Much of this work has focused on the role of the plate boundary, inherited weakness zones in the crust, or the role of decoupling along throughgoing weak layers (Willingshofer and Sokoutis, 2009; Luth et al., 2010; Sokoutis and Willingshofer, 2011; Calignano et al., 2015a, 2015b). The work of Sokoutis et al. (2005) is particularly germane to the present study. This work utilized different geometries to test overall lithospheric structure during shortening, but with a specific focus on whether a vertical boundary between juxtaposed lithospheres made a significant difference in the observed structure. The most important observation they noted is that folding in the mantle created uplift in the upper crust that localized above the inflection points in the folded mantle. Of particular relevance is the three-layer model (OCR-SL 17) that represented a cold lithosphere with a relatively strong mantle (e.g., Archean crust). Figure 5 is a line drawing of that experiment, wherein five zones of crustal uplift formed over two zones of mantle uplift. The vergence of the crustal uplift sometimes is synthetic with the sense of the uplifted Moho in some, but not all, cases. The experimental results suggest that crustal vergence may match but can differ from the vergence of mantle uplift.

Sokoutis et al. (2005) quantified wavelengths of mantle folding (λ_1) versus crustal deformation (λ_2), and the results of their study are shown in Figure 6A. The three-layer model (OCR-SL 17), which represented a cold lithosphere with a relatively strong mantle, resulted in a mantle wavelength of ~385 km and upper-crustal wavelength of ~165 km. We fit a line to all the data from that paper (Fig. 6). We, however, eliminated a single outlier point (displayed on the plot) for model OCR-SL 18, because it contained a weak layer embedded in the crust; in all other ways, it was identical to the other models. Note also that the physical experiments utilized two basic geometries, and hence the points form two clusters.

Figure 6 shows a very strong correlation using a least squares analysis (R = 0.96), and it indicates a linear relationship of 0.33 (with an intercept of 26 km). Using this relation, we plotted the wavelength of upper-crustal uplift and the wavelength of lithospheric mantle folding (Fig. 6B) for the case where deformation is controlled by lithospheric mantle buckling. In this scenario, upper-crustal folding can occur in addition to lithospheric mantle folding (Fig. 4).

It is important to note that the analog models are scaled for the different strengths of lithospheric layers. Thus, the lithospheric mantle appears to be thin (~1/3) relative to the thickness of a typical mantle lithosphere, such as that inferred for Wyoming. The reason is that the strength of the lithospheric mantle is thought to develop dominantly in its uppermost part; the load-bearing layer (which controls the wavelength and style of deformation) has a thickness that is only approximately one third of the total thickness of the mantle lithosphere (e.g., Burov and Watts, 2006). Below this depth, the mantle lithosphere does not have significant strength. Thus, the analog models must model the uppermost lithospheric mantle in a different way from the remainder of the lithospheric mantle (more "asthenospheric").

The second relevant work of recent analogue modeling results from the presence of a weak zone within a plate subjected to a horizontal end load. Willingshofer et al. (2005) and Sokoutis

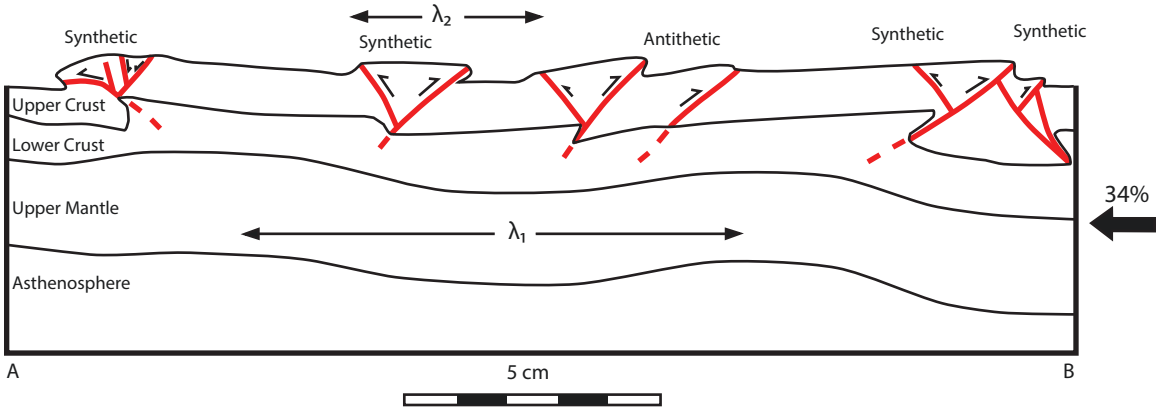

Figure 5. Line drawing of the scaled analog experiments by Sokoutis et al. (2005) for a three-layer model that simulates a cold lithosphere with a relatively strong mantle (OCR-SL 17). The mantle shows a preferred wavelength of folding that scales to ~385 km, but the upper crust deforms at wavelengths of ~165 km. The difference is that the upper crust deforms at the inflection points of the mantle folds, and it does not mimic the shape of the Moho. Further, the vergence of the upper-crustal deformation can be either synthetic or antithetic to the vergence of underlying mantle. Note that the analog experiments require only a thin "lithospheric" mantle, because the strength of the upper mantle is interpreted to lie only in this region.

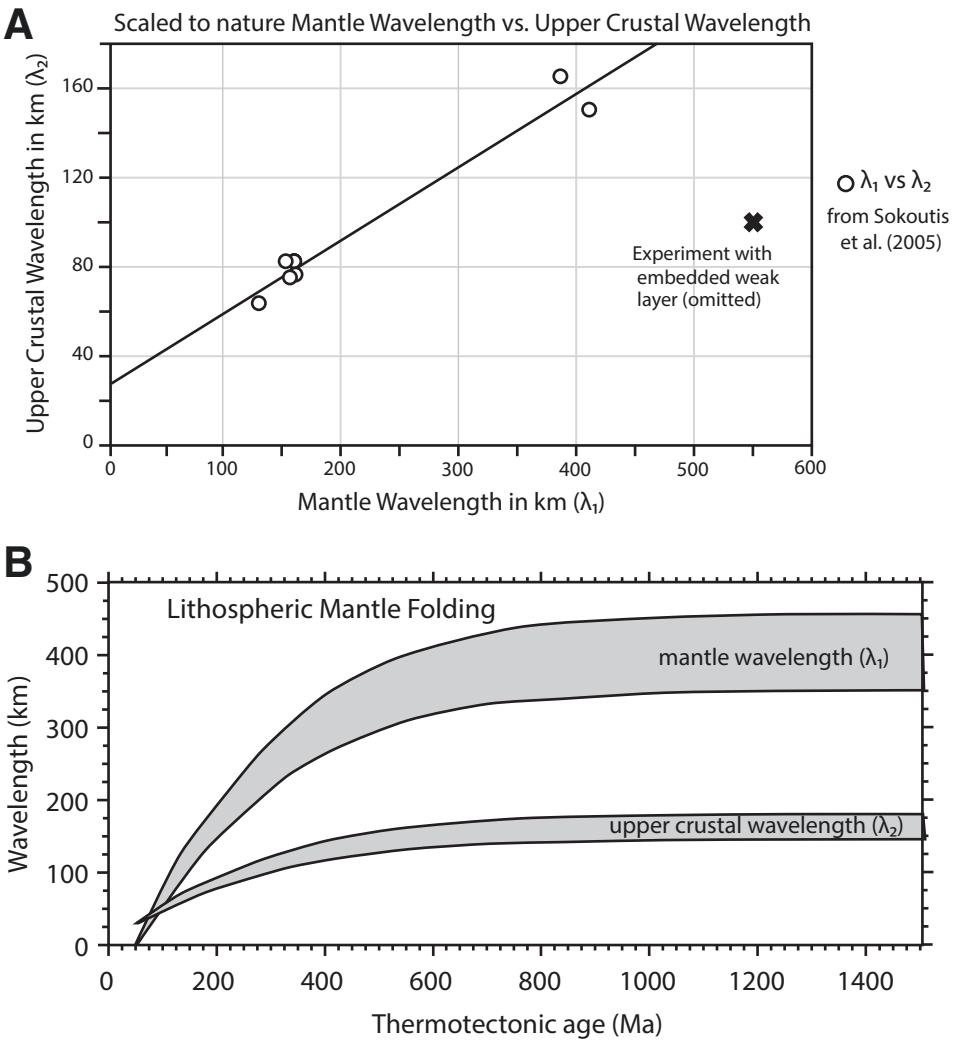

Figure 6. (A) Graph of scaled mantle wavelength (λ_1) to scaled upper-crustal deformation wavelength (λ_2), using the data produced by Sokoutis et al. (2005). Most data lie along a linear regression (R = 0.96), except for one experiment that contained an embedded weak layer (and was excluded from the analysis; see text). The wavelength of crustal deformation is approximately one third (+ 26 km intercept) of the mantle wavelength. (B) Results of this analysis applied to only the mantle lithosphere folding of Cloetingh et al. (1999). The mantle wavelength remains the same, but the upper-crustal wavelength is now shown; the distance off the x axis is because of the intercept of the line. Spacing of uplifts from Wyoming (~150–200 km; Tikoff and Maxson, 2001; Erslev, 2005), assuming thermotectonic age older than 600 Ma, are broadly consistent with this model.

and Willingshofer (2011) used multiple different geometries of a weak plate between two strong lithospheres (Fig. 7). They characterized this weak zone as a plate boundary, but it could also be considered as the presence of a preexisting suture or inherited crustal-scale structure within a foreland region subjected to an end load. This latter interpretation is particularly important if the Bighorns uplift was localized upon an Archean (to the west)–Proterozoic (to the east) tectonic boundary (Worthington et al., 2016; see Fig. 2A herein). Figure 7 shows line drawings of three relevant diagrams from the study of Sokoutis and Willingshofer (2011). In their model A1, a wide and symmetrical zone of weakness is placed in the middle of their model crust (Fig. 7A). While no detachment developed, the presence of a weak zone focuses the contractional deformation (Fig. 7B). Model A2 introduces a low-viscosity (weak) zone in the lowermost crust (Fig. 7C), equivalent to the position of the 7.x layer observed below the Bighorn uplift (Fig. 2B; Worthington et al., 2016). This weak zone localizes deformation at ~10% shortening, resulting in a strongly east-vergent structure (Fig. 7D). The final model (B2) places an asymmetrical weak zone at lower-crustal depths but with a 30° dip (Fig. 7E). This weak zone causes decoupling and asymmetric thrusting that is synthetic with the original dip of the weak zone (Fig. 7F). An interesting side effect of this model is that the degree of deformation of the adjacent "lithospheres" is reduced. The implication of the models is that the presence of a preexisting structural weakness in the crust can control the vergence of a structure. That information, combined with the results of Sokoutis et al. (2005), which indicate that crustal deformation occurs over the inflection points of mantle folding, will be relevant to consideration of the applicability of these models to the Bighorn uplift.

DISCUSSION

We agree with the assessments of Yeck et al. (2014) and Worthington et al. (2016), who stated that the new seismological data that reveal the Moho geometry of the Bighorn uplift eliminate the domino-style fault blocks at lithospheric scale (model 1

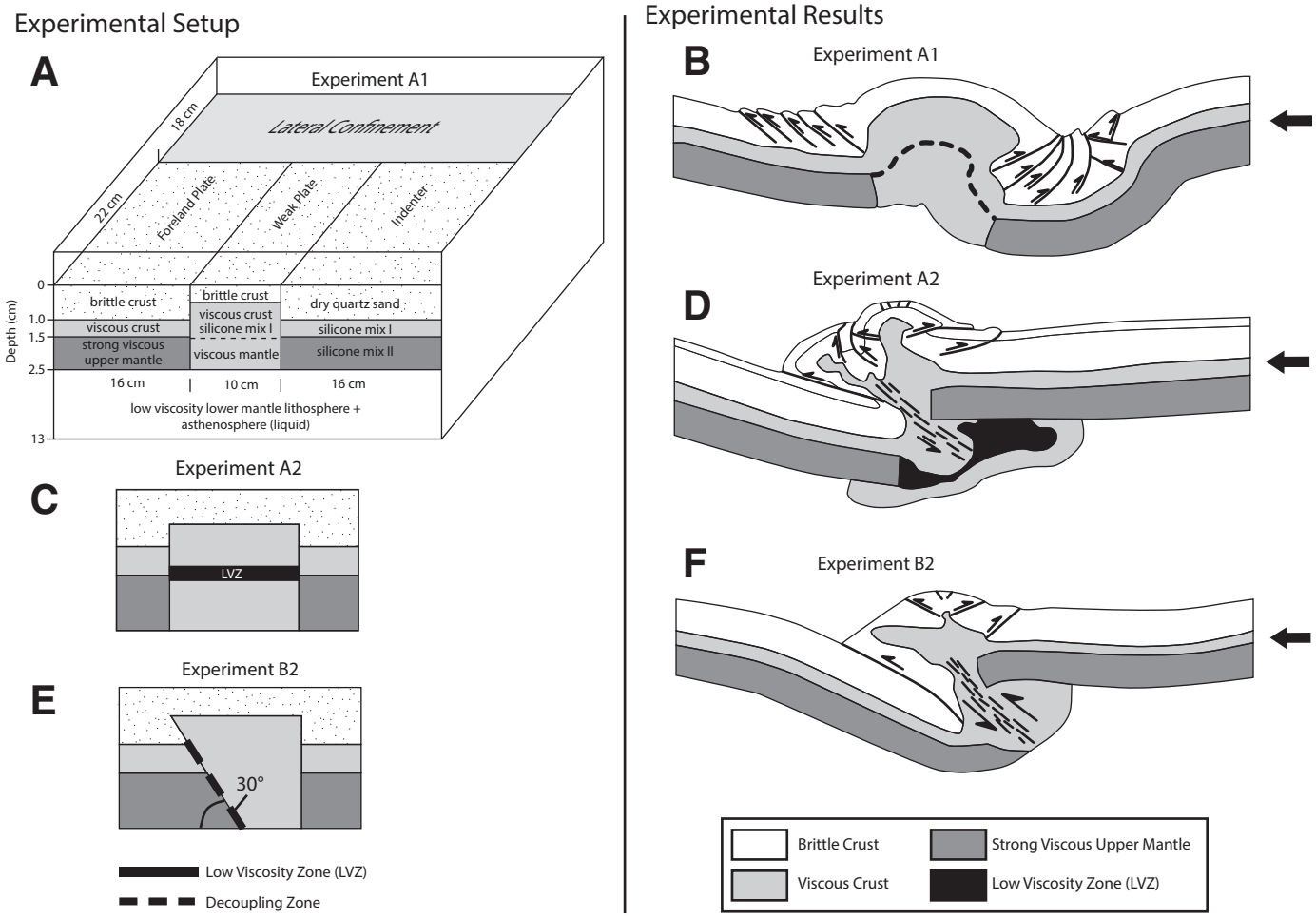

Figure 7. Experimental setup and scaled analog experiments from Sokoutis and Willingshofer (2011; also Willingshofer et al., 2005). These models investigated the role of a low-viscosity zone in various lithospheric positions and geometries. (A–B) Low-viscosity zone in the middle crust focused contractional deformation, but in a symmetrical manner. (C–D) Low-viscosity zone in the lowermost crust focused contractional deformation in an asymmetrical manner. (E–F) Thin, preexisting, and dipping suture focuses shear along that boundary, influencing deformation in the entire lithosphere.

in Fig. 2B; McQueen and Beaumont, 1989) and the pure shear lithospheric shortening and thickening (model 2 in Fig. 2B; Kulik and Schmidt, 1988; Egan and Urquhart, 1993) hypotheses. The two remaining hypotheses for Laramide uplift of the Bighorn uplift are: (3) crustal detachment (Erslev, 1993; Worthington et al., 2016); and (4) lithospheric folding (Tikoff and Maxson, 2001). The teleseismic receiver function analysis of Yeck et al. (2014) noted that either a deep crustal detachment system or lithospheric folding can explain the observed seismic results, although they favored the former. Using active-source P-wave velocity models, Worthington et al. (2016) took the same position, but they favored a detachment model for formation of the Bighorn uplift because of a perceived lack of correspondence of Moho topography and basement relief, crustal thickening across the uplift, and presence of low-velocity upper-crustal bodies. They did note the absence of clear seismological evidence for a subhorizontal detachment fault in the P-wave velocity data.

Results from the Bighorn EarthScope project, including the lack of evidence for detachment horizon(s), do not rule out a lithospheric folding mechanism for development of the Bighorn uplift. Further, deformation of the Rocky Mountain foreland has not been examined within the context of advances in understanding of foreland lithospheric deformation from scaled, analog experiments. Finally, it is worth noting that the "buckle" geometry proposed by Tikoff and Maxson (2001) is not correct in detail when applied to the Bighorn uplift. Drawing upon lithospheric folding research published since 2001 (e.g., Sokoutis et al., 2005; Willingshofer et al., 2005; Willingshofer and Sokoutis, 2009; Sokoutis and Willingshofer, 2011; Cloetingh and Burov, 2011; Calignano et al., 2015a, 2015b) and the results of the Bighorn Project, we explored whether lithospheric folding remains a viable mechanism that can successfully explain the crustal- and lithospheric-scale characteristics of the Bighorn uplift, and the seismological data. The mechanism has not been explored nor

reevaluated for Laramide uplifts of the Rocky Mountains since it was hypothesized by Tikoff and Maxson (2001; also Mederos et al., 2005).

Application of the Lithospheric Folding Model to the Results of the EarthScope Bighorn Data

Three major findings of the Bighorn seismic experiment (Yeck et al., 2014; Worthington et al., 2016) are as follows. (1) Teleseismic receiver function and P-wave velocity data both show a Moho geometry that deviates significantly from a flat-lying geometry under the present-day Bighorn uplift. (2) The single largest feature is the relief on the Moho from depths of ~50 km in the west to 37 km in the east, with the Bighorn uplift situated above an inflection point in the Moho geometry. (3) There is no major fault that offsets the Moho. These observations allow proposed models 1 and 2 for the Bighorn uplift to be ruled out, and all constitute evidence in favor of a lithospheric folding model (Fig. 2B). They accord with the scaled, three-layer analog models of Sokoutis et al. (2005) (Fig. 2C), which show significant crustal offset despite a lack of any Moho offset, and which display uplift exactly at the inflection point in terms of Moho uplift (cf. Tikoff and Maxson, 2001).

Drawing upon the higher-resolution, 3-D lithospheric structural data that now exist for the Bighorn Mountains region, a robust test of the lithospheric folding hypothesis can be made by examining arguments presented in favor of a crustal detachment mechanism (model 3, Fig. 2B). These are: (1) The shallowest Moho does not occur underneath the arch, but rather to the NE end of the broadband seismic array (Yeck et al., 2014). (2) At the position of the shallowest Moho, below the Powder River Basin, the Phanerozoic rocks are relatively flat-lying (Worthington et al., 2016). (3) The Moho geometry does not have an exact correspondence to the crustal structure of the Bighorn uplift that is delineated by the pattern of the Tensleep Formation (Yeck et al., 2014; Worthington et al., 2016). (4) The ~3 km domal uplift in the Moho is somewhat symmetric and thus cannot account for the east-vergent Bighorn structure (Worthington et al., 2016).

We counter these arguments in order. The scaled physical models of lithospheric folding do not produce upper-crustal uplifts that spatially correspond to the mantle uplift (except in the case of whole mantle folding; e.g., Sokoutis and Willingshofer, 2011). For example, highest crust/mantle relief in the experiment of Sokoutis et al. (2005) occurred in places of flat-lying sediments in the experimental models, bounded by uplifts. This implies that a spatial correspondence of shallowest Moho with an upper-mantle inflection is not essential to the mechanism of lithospheric folding. The argument that the Moho geometry does not correlate to the crustal structure of the uplift is also consistent with the models of lithospheric folding (Fig. 5). This effect is seen in most models of lithospheric folding (e.g., Martinod, 1991).

Another argument concerns the lack of a predicted E-vergence of the Bighorn uplift, given the Moho geometry (Worthington et al., 2016). However, no set vergence (for the geometry of the Moho inflection point) is evident from the experiments of Sokoutis et al. (2005). It is not apparent from the scaled physical models that the vergence of the mantle uplift controls the crustal vergence (Fig. 5). Worthington et al. (2016) interpreted that a preexisting, E-dipping Proterozoic boundary controls the east side of the Bighorn uplift. We view this feature to be a crustal manifestation of the effect of a preexisting weakness, such as those in the physical experiments of Willingshofer et al. (2005) and Sokoutis and Willingshofer (2011), which show that dipping weak zones get reactivated during crustal deformation (Fig. 7), likely because the anisotropy is transmitted throughout the lithosphere. The scaled analog models predict that a preexisting lithospheric-scale boundary, such as occurs in the eastern Bighorns Mountains, can have a role in the nucleation of the lithospheric buckling. Further, this type of feature can affect the upper-crustal vergence, regardless of the uplift direction at the Moho. Figure 2C shows that there are two Moho geometries, based on the results of Sokoutis et al. (2005), that would cause uplift in the presence of a strong, preexisting boundary.

The Bighorn basement surface is asymmetric with a NE vergence (e.g., Worthington et al., 2016). The form of the ~3 km domal uplift in the Moho, situated approximately below the surface expression of the Bighorn uplift, is more symmetric. A possible explanation for why that low-amplitude (~3 km) bulge exists is suggested by the crustal seismic results of Worthington et al. (2016), which identified a dense layer of lowermost crust—the 7.x layer—on either side of the Bighorn range that is absent where the Moho is uplifted. The scenario most resembles experiment A2 (or A1) of Sokoutis and Willingshofer (2011), which resulted in extreme behavior due to the major contrasts between viscous materials used in the modeling, resulting in a localization of deformation upon a weak layer in the deep crust and relative uplift of the top of the lithospheric model (see Fig. 7). The contrast in rheological behavior of "standard" lower crust versus "7.x" lower crust is likely to be significantly less pronounced than that introduced in the analog models, but the absence of the 7.x layer underneath the Bighorn uplift could have been a factor in the development of a "dome" in the local Moho.

Regional Context for the Bighorn Mountains Transect

The mantle below the Bighorn uplift is folded at a wavelength much larger than that covered by the seismic data of the Bighorn experiment, consistent with the predictions of Cloetingh et al. (1999), which indicated that the Wyoming province should display strong, cold behavior. The recent synthesis of low-temperature thermochronology data for the Bighorn and Wind River ranges clearly shows that the region's crystalline basement cooled during the Precambrian and has been stable since Neoproterozoic time (e.g., Orme et al., 2016). The low amplitude and wide, regular spacing of the Wind River, Bighorn, and Black Hills uplifts (Figs. 8 and 9) are expressions of cold, stiff lithosphere.

The lithospheric flexure beneath the Bighorn Mountains and Basin continues southwest into the Wind River uplift of western

Wyoming, where the Moho elevation varies from 52 km depth on the NE side of the Wind River Mountains (beneath the Wind River Basin) to 38 km depth on the SW side (Groshong and Porter, 2019). Similar to the Bighorn uplift, the Wind River uplift occurs near the inferred inflection point of the Moho. Also similar to the Bighorn uplift, the crustal west-vergent Wind River Mountain range has the opposite vergence to the Moho geometry.

The amount of Moho relief below the Wind River Mountains is comparable to the variation in Moho elevation on either side of the Bighorn Mountains, although with the opposite geometry. The study by Groshong and Porter (2019) did not obtain significant broadband coverage to produce a Moho image continuous into the Bighorn Project transect. Therefore, we used the seismic results of Gilbert (2012, B–B′ line of that study) to connect the ~50-km-deep Moho on the NE side of the Wind River Mountains into the ~50-km-deep Moho on the SW wide side of the Bighorn uplift, as depicted in Figure 8. Further, the Moho continues to be shallow eastward under the Powder River Basin (Gilbert, 2012). The wavelength of the crustal uplifts is ~200 km, and the wavelength of the mantle is ~450 km. These wavelengths are consistent with those calculated for lithospheric folding of cold, strong lithosphere by Cloetingh et al. (1999).

At this length scale, the lithospheric folds that exist under the eastern Rocky Mountains finally become apparent (Fig. 8). Between the Wind River uplift and the Bighorn uplift, the center of the mantle syncline at ~50 km depth exists somewhere beneath the Wind River/Bighorn Basins. The center of mantle anticline east of the Bighorn uplift and west of the Black Hills exists under the Powder River Basin. The E-W–trending Owl Creek Mountains uplift was omitted from consideration because it arose as a left-lateral accommodation structure localized by Precambrian fabrics (see Paylor and Yin, 1993; Bader, 2018) and appears to have no genetic relation to the proposed lithospheric folding.

The 70 km spacing of the EarthScope Transportable Array provides a continent-scale view of crustal thickness through the use of Ps receiver functions (e.g., Gilbert, 2012; Schmandt et al., 2015; Thurner et al., 2015). Most of these studies discuss results in terms of crustal thickness, although we postulate that the current crustal thickness is not an inherent feature of the lithosphere but rather partly a result of deformation; hence, we recast these results in terms of depths of the Moho. Further, we did not use the lithosphere-asthenosphere boundary in Wyoming, determined from seismic studies, in our analysis for two reasons. First, the strength of the upper mantle exists dominantly in the upper ~40 km of the lithospheric mantle. Hence, the geometry of the lithosphere-asthenosphere boundary is largely nondiagnostic of lithospheric folding models. Second, the lithosphere-asthenosphere boundary in Wyoming is likely to have been modified after the Late Cretaceous by a combination of small-scale convection, proposed slab subduction, and the encroaching Yellowstone hotspot (e.g., Dave and Li, 2016).

We conclude that the Bighorn seismic data support the lithospheric folding model well, and that lithospheric folding is a viable mechanism that can explain the formation of Laramide foreland uplifts.

Issues to Be Addressed by Crustal Detachment Models

The 2009–2011 Bighorn Project active-source experiment produced superb seismic reflection data (Worthington et al., 2016), achieved as a result of significant improvement in seismic reflection techniques since the late 1970s, when COCORP surveys were conducted in Wyoming (e.g., Smithson et al., 1979). The project employed active seismic techniques that are best suited for detection of shallowly dipping structures with major offset; however, a detachment structure was not apparently imaged beneath the Bighorn uplift (Worthington et al., 2016, p. 233). By contrast, active seismology applied to the Wind River uplift does clearly show a shallowly E-dipping crustal reflector that is laterally extensive for at least 25 km (Smithson et al., 1979). Seismic evidence for low-angle structure is lacking, but it is the single most critical observation that could substantiate the crustal detachment mechanism for formation of the Bighorn Mountains uplift.

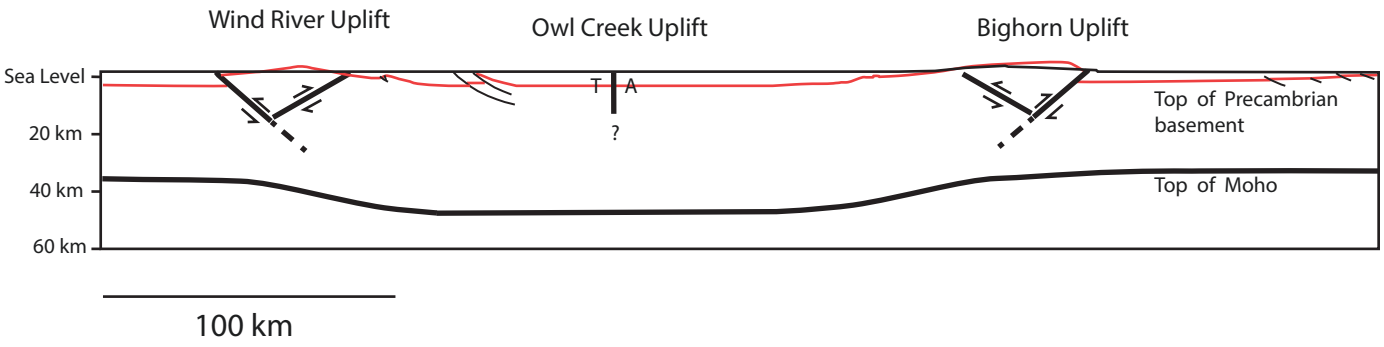

Figure 8. Interpretive cross section from the Wind River uplift to the Bighorn uplift, in order to show the wavelength of a lithospheric buckle and how it relates to surface uplift in Wyoming. Compare with the results of the analog experiments (Fig. 5). T—towards and A—away as applied to the sinistral strike-slip fault. Moho geometry in Bighorn region is from Yeck et al. (2014) and Worthington et al. (2016); that from below Wind River uplift is from Groshong and Porter (2019). The results are consistent with results from western United States of Gilbert (2012).

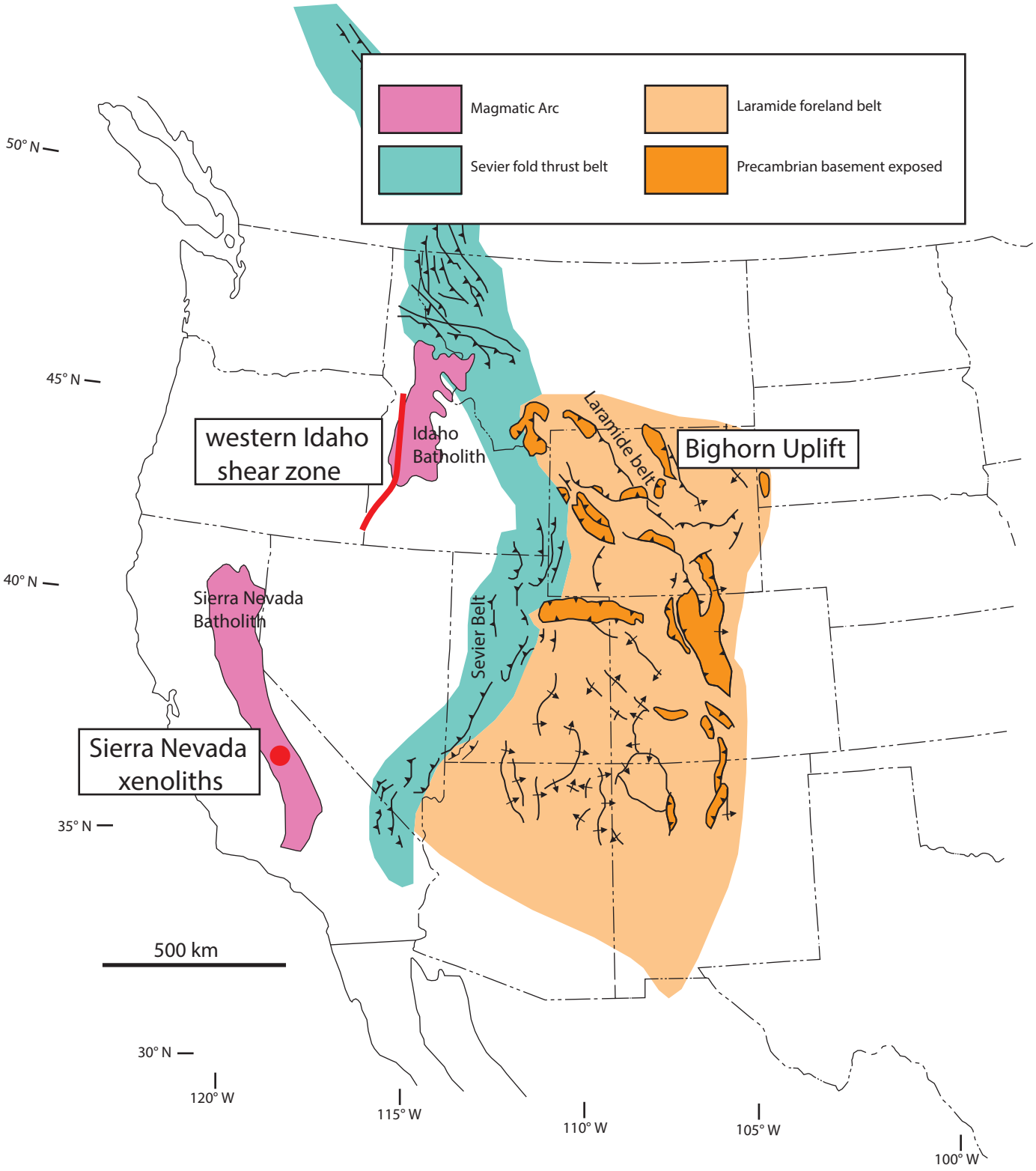

Figure 9. Map of the U.S. portion of the North American Cordillera, modified from Burchfiel et al. (1992) and Weil and Yonkee (2012). The lines with arrows indicate fold axes and vergence direction, respectively, of the Laramide-style block uplifts. The reverse fault symbols (lines with triangles) designate the position of some of the main thrust faults of the Sevier fold-and-thrust belt. The position of the western Idaho shear zone (red line) and the position of eclogitic mantle xenoliths in the Sierra Nevada (red dot) are two piercing points that require that the crust and mantle were coupled throughout much of the Sevier-Laramide orogeny. Crustal detachment did occur within the Sevier fold-and-thrust belt, presumably related to crustal thickening in the hinterland of the orogen (Nevadaplano).

A geometric requirement of the crustal detachment mechanism (model 3, Fig. 2B) is that the curved fault surfaces of the Bighorn uplift should cause systematic rotation if there are changes in displacement along fault strike. Vertical axis rotations would occur, which should be reflected by paleomagnetic vectors (e.g., Yonkee and Weil, 2010). The Bighorn Mountains must have along-strike gradients in displacement because the structure is of limited along-strike extent. However, vertical axis rotation is not observed (Weil et al., 2014), a finding that suggests a coupled crustal section.

The Precambrian suture/tectonic boundary that localized the eastern edge of the Bighorn uplift (Worthington et al., 2016) presents another problem for the crustal detachment hypothesis. If a crustal detachment was responsible for the Rocky Mountain uplifts, that detachment must continue northeastward to the Black Hills uplift (and Hartville uplift; Fig. 1). At the east edge of the Bighorn uplift, however, crust that lacks the 7.x layer is juxtaposed against crust that contains the 7.x layer, and so the structure does not allow sufficient lateral continuity for there to be a significant detachment fault. The Laramide-active orogenic-scale crustal detachment would have to abruptly terminate on the east side of the Bighorn uplift, and it could not be the controlling structure for the Black Hills, Hartville, or Chadron uplifts, further east.

To the west, at the (Laramide) continental margin in both Idaho and California, there is evidence against the presence of a throughgoing crustal detachment (Fig. 9). The IDOR EarthScope project studied the western margin of North America in western Idaho (Tikoff et al., 2017), focusing upon the western Idaho shear zone, a transpressional shear zone active at 100–85 Ma (Giorgis et al., 2008; Braudy et al., 2017). The western Idaho shear zone demarcates the abrupt contact between the North American plate and the accreted terranes of the Blue Mountains. The crustal portion of the western edge of North America directly overlies the mantle boundary, according to seismic studies that identify an ~8 km Moho offset across the vertical western Idaho shear zone (e.g., Stanciu et al., 2016; Davenport et al., 2017). Had there been relative displacement upon a crustal-scale detachment during the Laramide orogeny, a deflection within the crust would be observed.

The coherence of the crustal column in Idaho is validated by multiple magmatic centers that were active since the formation of the western Idaho shear zone and that display clear geochemical connections to the lithospheric mantle below, be it continental or oceanic in origin (Gaschnig et al., 2010, 2011; Kurz et al., 2017). A crustal detachment model requires that the crust has moved relative to the underlying mantle across a vast region (e.g., Oldow et al., 1989). This prediction was explicitly made for the Idaho margin by Leeman et al. (1992) and was one of the proposed hypotheses of the IDOR project (Tikoff et al., 2017), but the western Idaho shear zone provides a lithospheric pinning point unaffected by crustal translation.

The same argument can be made for the California margin (Fig. 9), where the eclogitic root beneath the Sierra Nevada batholith (Ducea and Saleeby, 1996, 1998) provides a lithospheric pinning point. This eclogitic root must have extended to at least 130 km below the Sierra Nevada arc in order to have provided a source for Cretaceous-aged eclogitic mantle xenoliths brought up in Miocene volcanics in the Sierra Nevada. The spatial connection would have been disrupted had there been displacement on a throughgoing crustal detachment. Thus, to propose a crustal detachment model, one must consider the "out of the field area" considerations. Oldow et al. (1989), in one of the clearest explanations of the orogenic float idea, explicitly noted that the detachment must go back to the plate boundary.

A final issue for the crustal detachment mechanism for the Bighorn and other foreland uplifts is the discovery that the initiation of basement uplift occurred at ca. 100 Ma in the northern Rocky Mountains, determined by low-temperature thermochronology (Carrapa et al., 2019). The new data corroborate evidence for pre-Paleogene uplift in specific ranges (e.g., Wind River Range; Steidtmann and Middleton, 1991). The onset of deformation is now known to temporally correlate to—and likely resulted from—deformation associated with the western Idaho shear zone plate boundary (Carrapa et al., 2019). Deformation recorded by early calcite veins from the Bighorn Basin, newly dated by U-Pb methods at ca. 85 Ma (Beaudoin et al., 2018; also see Beaudoin et al., 2019, reply), falls within this earlier deformation phase and cannot be associated with a throughgoing crustal detachment.

In summary, the Bighorn Project did not produce definitive evidence of a crustal detachment below the Bighorn uplift, and the model is contradicted by regional constraints.

Terrane Collision or Flat-Slab Subduction?

The National Science Foundation EarthScope program greatly advanced the understanding of the extent and evolution of lithosphere in the western United States, bringing new insight into the underlying cause for formation of the Laramide block uplifts. If one accepts that foreland deformation was the result of an end load on the western margin of North America due to plate convergence, there are two possible models for the origins of the end load. The prevailing view is that shallow slab subduction on the western coast of North America along the California margin resulted in inland deformation. This concept was first proposed by Dickinson and Snyder (1978), although it has received some significant modifications (e.g., Saleeby, 2003). Axen et al. (2018) used numerical models to illustrate that shallow slab subduction likely results in end loading. Most models for shallow subduction in Cretaceous–Paleogene time do not include the Idaho segment of the orogeny, and the geology of Idaho is incompatible with that model.

The alternative is terrane collision, in particular, the collision of the Insular terrane block, which is considered to have driven the development of the western Idaho shear zone (e.g., Giorgis et al., 2008). The new recognition that early Laramide-style block uplifts in Montana initiated during movement on the western Idaho shear zone (Carrapa et al., 2019) introduces the possibility that terrane collision was responsible for block

uplifts ca. 100 Ma in the northern Rocky Mountains. The Rock Springs uplift of southern Wyoming, associated with syn-uplift deposition that provides timing, also shows evidence for uplift at ca. 95 Ma (Mederos et al., 2005). This contemporaneity of foreland block uplifts with terrane collision suggests that the initial movement on block uplifts in the northern Rocky Mountains resulted from the Insular terrane end load on the western edge of North America.

Either proposed mechanism for formation of the Rocky Mountains results in an end load on the western edge of North America, and it is permissible that both acted in sequence, with an earlier phase (100–85 Ma) of end load produced by terrane collision and a later phase (80–55 Ma) of end load resulting from shallow subduction in the northern Rocky Mountains. Alternatively, the end load in the northern Rockies could have arisen solely from terrane collision, as shallow slab subduction cannot apply in the northern region at 100 Ma.

CONCLUSIONS

The EarthScope Bighorn Project was conceived as a test between four hypotheses for the development of basement-cored block uplifts that occur in the eastern Rocky Mountains (Yeck et al., 2014; Worthington et al., 2016). These models—applied to the Bighorn uplift—were: (1) lithospheric fault blocks, (2) lower-crustal pure shear thickening, (3) crustal detachment, and (4) lithospheric folding (buckling). No model envisioned in the initial stages of the project matched the primary observation determined from the active-source seismic data: a Moho that steps from 50 km deep below the Bighorn Basin on the west to 37 km deep below the Powder River Basin to the east. The lack of a discrete offset on the Moho or a depressed Moho rules out the lithospheric fault blocks and pure shear thickening models, respectively. The absence of clearly imaged detachment faults beneath the Bighorn arch and the Bighorn Basin, and the prohibitive regional relationships that indicate the lithospheric mantle is generally coupled to the crust to both east and west are counter to the crustal detachment model. The crustal detachment model has regional geological problems and major mechanical problems associated with moving large sections of crust over large distances on subhorizontal surfaces.

In this contribution, we argue that lithospheric buckling modeling satisfactorily explains the results of the Bighorn Project and other regional studies in the following ways:

1. The Bighorn uplift occurs at an inflection point in the low-amplitude folding of the lithospheric mantle (Burg et al., 1994). The scaled models of Sokoutis et al. (2005), particularly those designed to mimic a cold and strong lithosphere, are a compelling match to the Bighorn seismic results.
2. The vergence of the Bighorn uplift is controlled by the existence of a Proterozoic suture zone, which correlates with the eastern side of the Bighorn uplift. Even in scaled lithospheric buckling models without preexisting structures, the vergence of the folding may be either synthetic or antithetic to the Moho uplift (Sokoutis et al., 2005). However, in cases in which a preexisting weakness is introduced into scaled models, those models are preferentially reactivated by lithospheric folding (e.g., Sokoutis and Willingshofer, 2011).
3. Lithospheric folding explains the arch-like geometry of the uplifts, as the Laramide-style block uplifts are epiphenomena on folds in the lithospheric mantle. In Wyoming, the spacing (wavelength) for the upper-crustal deformation is ~150–200 km (Tikoff and Maxson, 2001; Erslev, 2005). Combining the Bighorn results with recent results from the Wind River uplift (Groshong and Porter, 2019), the folded mantle wavelength is ~450 km (e.g., the mantle anticline is located below the Powder River Basin, and the mantle syncline is below the Wind River Basin). The expected folding wavelength of mantle folding for an old, cold, and strong lithospheric mantle is ~400–450 m (Cloetingh et al., 1999). Because upper crust deforms at the inflection point, it deforms at a wavelength that is approximately one third (+ 26 km intercept) of the mantle folding, i.e., 156–175 km, in accord with observations.
4. Lithospheric folding in the foreland provides an explanation for the major differences in shortening direction found in the Sevier fold-and-thrust belt (e.g., Yonkee and Weil, 2010) and the basement-cored uplifts (e.g., Weil et al., 2014). The orientations of the Sevier fold-and-thrust belt result from orographic-determined deformation on a detached system, whereas the shortening direction for the Laramide uplifts results from mantle-guided stresses consistent with an end load.
5. Arch-like, basement-cored uplifts during the Cretaceous–Paleogene are not limited to Wyoming, but are also found in the High Plains, Colorado Plateau, and western Montana. Lithospheric folding is a viable mechanism for foreland deformation in all these regions.

In summary, the EarthScope Bighorn Project proposed to investigate the Bighorn Mountains in order to determine how basement-cored block uplifts formed in the Sevier foreland. The Bighorns data, together with other regional constraints, are consistent with a lithospheric buckling model, a result that is possibly extendable to other parts of the eastern Rocky Mountains and High Plains.

ACKNOWLEDGMENTS

We thank all the principal investigators and participants in the EarthScope Bighorn Project for their multiyear effort, which provided superb data of sufficient resolution to test long-standing hypotheses. We particularly thank M. Anderson and L. Worthington for their open-mindedness to consider alternative models. National Science Foundation grant EAR-0843889 supported Colorado College investigators. Ellen M. Nelson is

acknowledged for her contributions to manuscript preparation and figure drafting. Ryan Porter, David Malone, and two anonymous reviewers provided very helpful reviews that allowed us to improve the presentation. We are grateful to the editors of this volume for the opportunity to update and examine a lithospheric folding model for the Bighorn uplift.

REFERENCES CITED

Axen, G.J., van Wijk, J.W., and Currie, C.A., 2018, Basal continental mantle lithosphere displaced by flat-slab subduction: Nature Geoscience, v. 11, p. 961–964, https://doi.org/10.1038/s41561-018-0263-9.

Bader, J.W., 2018, Structural inheritance and the role of basement anisotropies in the Laramide structural and tectonic evolution of the North American Cordilleran foreland, Wyoming: Lithosphere, v. 11, p. 129–148, https://doi.org/10.1130/L1022.1.

Beaudoin, N., Lacombe, O., Bellahsen, N., Amrouch, K., and Daniel, J.-M., 2014, Evolution of pore-fluid pressure during folding and basin contraction in overpressured reservoirs: Insights from the Madison-Phosphoria carbonate formations in the Bighorn Basin (Wyoming, USA): Marine and Petroleum Geology, v. 55, p. 214–229, https://doi.org/10.1016/j.marpetgeo.2013.12.009.

Beaudoin, N., Lacombe, O., Roberts, N.M.W., and Koehn, D., 2018, U-Pb dating of calcite veins reveals complex stress evolution and thrust sequence in the Bighorn Basin, Wyoming, U.S.A.: Geology, v. 46, no. 11, p. 1015–1018, https://doi.org/10.1130/G45379.1.

Beaudoin, N., Lacombe, O., Roberts, N.M.W., and Koehn, D., 2019, U-Pb dating of calcite veins reveals complex stress evolution and thrust sequence in the Bighorn Basin, Wyoming, USA: Reply: Geology, v. 47, no. 9, p. e481, https://doi.org/10.1130/G46606Y.1.

Biot, M.A., 1965, Mechanics of Incremental Deformations: New York, John Wiley & Sons, 504 p.

Bird, P., 1988, Formation of the Rocky Mountains, western United States: A continuum computer model: Science, v. 239, p. 1501–1507, https://doi.org/10.1126/science.239.4847.1501.

Brace, W.F., and Kohlstedt, D.L., 1980, Limits on lithospheric stress imposed by laboratory experiments: Journal of Geophysical Research, v. 85, p. 6248–6252, https://doi.org/10.1029/JB085iB11p06248.

Braudy, N., Gaschnig, R.M., Wilford, D., Vervoort, J.D., Nelson, C.L., Davidson, C., Kahn, M.J., and Tikoff, B., 2017, Timing and deformation conditions of the Western Idaho shear zone, West Mountain, west-central Idaho: Lithosphere, v. 9, no. 2, p. 157–183, https://doi.org/10.1130/L519.1.

Brown, W.G., 1993, Structural style of Laramide basement-cored uplifts and associated folds, *in* Snoke, A.W., Steidtmann, J.R., and Roberts, S.M., eds., Geology of Wyoming: Geological Survey of Wyoming Memoir 5, p. 312–371.

Burchfiel, B.C., Cowan, D.S., and Davis, G.A., 1992, Tectonic overview of the Cordilleran orogen in the western United States, *in* Burchfiel, B.C., Lipman, P.W., and Zoback, M.L., eds., The Cordilleran Orogen: Conterminous U.S.: Boulder, Colorado, Geological Society of America, Geology of North America, v. G-3, p. 407–479, https://doi.org/10.1130/DNAG-GNA-G3.407.

Burg, J.P., Davy, P., and Martinod, J., 1994, Shortening of analogue models of the continental lithosphere: New hypothesis for the formation of the Tibetan Plateau: Tectonics, v. 13, no. 2, p. 475–483, https://doi.org/10.1029/93TC02738.

Burg, J.-P., Sokoutis, D., and Bonini, M., 2002, Model-inspired interpretation of seismic structures in the central Alps: Crustal wedging and buckling at mature stage of collision: Geology, v. 30, p. 643–646, https://doi.org/10.1130/0091-7613(2002)030<0643:MIIOSS>2.0.CO;2.

Burov, E.B., and Watts, A.B., 2006, The long-term strength of continental lithosphere: "Jelly sandwich" or "crème brûlée"?: GSA Today, v. 16, no. 1, p. 4–10, https://doi.org/10.1130/1052-5173(2006)016<4:TLTSOC>2.0.CO;2.

Burov, E.B., Nikishin, A.M., Cloetingh, S., and Lobkovsky, L.I., 1993, Continental lithosphere folding in Central Asia: Part II. Constraints from gravity and tectonic modelling: Tectonophysics, v. 226, no. 1–4, p. 73–87, https://doi.org/10.1016/0040-1951(93)90111-V.

Calignano, E., Sokoutis, D., Willingshofer, E., Gueydan, F., and Cloetingh, S., 2015a, Asymmetric vs. symmetric deep lithospheric architecture of intraplate continental orogens: Earth and Planetary Science Letters, v. 424, p. 38–50, https://doi.org/10.1016/j.epsl.2015.05.022.

Calignano, E., Sokoutis, D., Willingshofer, E., Gueydan, F., and Cloetingh, S., 2015b, Strain localization at the margins of strong lithospheric domains: Insights from analogue models: Tectonics, v. 34, no. 3, p. 396–412, https://doi.org/10.1002/2014TC003756.

Carrapa, B., DeCelles, P.G., and Romero, M., 2019, Early inception of the Laramide orogeny in southwestern Montana and northern Wyoming: Implications for models of flat-slab subduction: Journal of Geophysical Research–Solid Earth, v. 124, no. 2, p. 2102–2123, https://doi.org/10.1029/2018JB016888.

Cloetingh, S., and Burov, E., 2011, Lithospheric folding and sedimentary basin evolution: A review and analysis of formation mechanisms: Basin Research, v. 23, no. 3, p. 257–290, https://doi.org/10.1111/j.1365-2117.2010.00490.x.

Cloetingh, S., Burov, E., and Poliakov, A., 1999, Lithosphere folding: Primary response to compression? (from central Asia to Paris basin): Tectonics, v. 18, no. 6, p. 1064–1083, https://doi.org/10.1029/1999TC900040.

Dave, R., and Li, A., 2016, Shear wave velocity and radial anisotropy beneath the Wyoming Craton: Craton destruction and lithospheric layering: Abstract T13C-2725 presented at 2016 Fall Meeting, AGU, San Francisco, California, 12–16 December.

Davenport, K.K., Hole, J.A., Tikoff, B., Russo, R.M., and Harder, S.H., 2017, A strong contrast in crustal architecture from accreted terranes to craton, constrained by controlled-source seismic data in Idaho and eastern Oregon: Lithosphere, v. 9, no. 2, p. 325–340, https://doi.org/10.1130/L553.1.

Davy, P., and Cobbold, P.R., 1988, Indentation tectonics in nature and experiment: 1. Experiments scaled for gravity: Bulletin of the Geological Institutions of the University of Uppsala, v. 14, p. 129–141.

Davy, P., and Cobbold, P.R., 1991, Experiments on shortening of a 4-layer model of the continental lithosphere: Tectonophysics, v. 188, p. 1–25, https://doi.org/10.1016/0040-1951(91)90311-F.

Dickinson, W.R., and Snyder, W.S., 1978, Plate tectonics of the Laramide orogeny, *in* Matthews, V., III, ed., Laramide Folding Associated with Basement Block Faulting in the Western United States: Geological Society of America Memoir 151, p. 355–366, https://doi.org/10.1130/MEM151-p355.

Dickinson, W.R., Klute, M.A., Hayes, M.J., Janecke, S.U., Lundin, E.R., McKittrick, M.A., and Olivares, M.D., 1988, Paleogeographic and paleotectonic setting of Laramide sedimentary basins in the central Rocky Mountain region: Geological Society of America Bulletin, v. 100, p. 1023–1039, https://doi.org/10.1130/0016-7606(1988)100<1023:PAPSOL>2.3.CO;2.

Doane, T., 2010, An Integrated Structural and Gravity Analysis: The Role of Lineaments in Laramide Deformation and Implications for Lithospheric Scale Response [Senior undergraduate thesis]: Colorado Springs, Colorado, Colorado College, 100 p.

Ducea, M.N., and Saleeby, J.B., 1996, Buoyancy sources for a large, unrooted mountain range, the Sierra Nevada, California: Evidence from xenolith thermobarometry: Journal of Geophysical Research, v. 101, p. 8229–8244, https://doi.org/10.1029/95JB03452.

Ducea, M.N., and Saleeby, J.B., 1998, The age and origin of a thick ultramafic keel from beneath the Sierra Nevada Batholith: Contributions to Mineralogy and Petrology, v. 133, p. 169–185, https://doi.org/10.1007/s004100050445.

Egan, S.S., and Urquhart, J.M., 1993, Numerical modelling of lithospheric shortening; Application to the Laramide orogenic province, western USA: Tectonophysics, v. 221, p. 385–411, https://doi.org/10.1016/0040-1951(93)90170-O.

Erslev, E.A., 1993, Thrusts, back-thrusts, and detachment of Rocky Mountain foreland arches, *in* Schmidt, C.J., Chase, R.B., and Erslev, E.A., eds., Laramide Basement Deformation in the Rocky Mountain Foreland of the Western United States: Geological Society of America Special Paper 280, p. 339–358, https://doi.org/10.1130/SPE280-p339.

Erslev, E.A., 2005, 2D Laramide geometries and kinematics of the Rocky Mountains, western USA, *in* Kalstrom, K.E., and Keller, G.R., eds., The Rocky Mountain Region: An Evolving Lithosphere: American Geophysical Union Geophysical Monograph 154, p. 7–20, https://doi.org/10.1029/154GM02.

Faugere, E., and Brun, J.P., 1984, Modelisation experimentale de la distention continentale: Comptes Rendus des Séances de l'Academie des Sciences, ser. 2, Mécanique, Physique, et Chimie, Sciences de l'Univers: Sciences de la Terre, v. 299, no. 7, p. 365–370.

Frost, C.D., and Fanning, C.M., 2006, Archean geochronological framework of the Bighorn Mountains, Wyoming: Canadian Journal of Earth Sciences, v. 43, no. 10, p. 1399–1418, https://doi.org/10.1139/e06-051.

Gaschnig, R.M., Vervoort, J.D., Lewis, R.S., and McClelland, W.C., 2010, Migrating magmatism in the northern US Cordillera: In situ U-Pb geochronology of the Idaho batholith: Contributions to Mineralogy and Petrology, v. 159, p. 863–883, https://doi.org/10.1007/s00410-009-0459-5.

Gaschnig, R.M., Vervoort, J.D., Lewis, R.S., and Tikoff, B., 2011, Isotopic evolution of the Idaho batholith and Challis intrusive province, northern US Cordillera: Journal of Petrology, v. 52, p. 2397–2429, https://doi.org/10.1093/petrology/egr050.

Gilbert, H., 2012, Crustal structure and signatures of recent tectonism as influenced by ancient terranes in the western United States: Geosphere, v. 8, no. 1, p. 141–157, https://doi.org/10.1130/GES00720.1.

Giorgis, S., McClelland, W., Fayon, A., Singer, B., and Tikoff, B., 2008, Timing of deformation and exhumation in the Western Idaho shear zone, McCall, Idaho: Geological Society of America Bulletin, v. 120, p. 1119–1133, https://doi.org/10.1130/B26291.1.

Groshong, R.H., and Porter, R., 2019, Predictive models for the deep geometry of a thick-skinned thrust matched to crustal structure: Wind River Range, western U.S.: Lithosphere, v. 11, no. 4, p. 448–464, https://doi.org/10.1130/L1031.1.

Hudleston, P.J., 1973, An analysis of single layer folds developed experimentally in viscous media: Tectonophysics, v. 16, p. 189–214, https://doi.org/10.1016/0040-1951(73)90012-7.

Humphreys, E., Hessler, E., Dueker, K., Farmer, G.L., Erslev, E., and Atwater, T., 2003, How Laramide-age hydration of North American lithosphere by the Farallon slab controlled subsequent activity in the western United States: International Geology Review, v. 45, p. 575–595, https://doi.org/10.2747/0020-6814.45.7.575.

Kennett, B.L.N., and Iaffaldano, G., 2012, Role of lithosphere in intracontinental deformation: Central Australia: Gondwana Research, v. 24, no. 3–4, p. 958–968, https://doi.org/10.1016/j.gr.2012.10.010.

Kirby, S.H., 1983, Rheology of the lithosphere: Reviews of Geophysics and Space Physics, v. 21, no. 6, p. 1458–1487, https://doi.org/10.1029/RG021i006p01458.

Kirby, S.H., 1985, Rock mechanics observations pertinent to the rheology of the continental lithosphere and the localization of strain along shear zones: Tectonophysics, v. 119, no. 1–4, p. 1–27, https://doi.org/10.1016/0040-1951(85)90030-7.

Kucks, R.P., and Hill, P.L., 2000, Wyoming Aeromagnetic and Gravity Maps and Data: A Web Site for Distribution of Data: U.S. Geological Survey Open-File Report 00-0198, https://greenwood.cr.usgs.gov/pub/open-file-reports/ofr-00-0198/html/wyoming.htm.

Kulik, D.M., and Schmidt, C.J., 1988, Regions of overlap and styles of interaction of Cordilleran thrust belt and Rocky Mountain foreland, *in* Schmidt, C.J., and Perry, W.J., Jr., eds., Interaction of the Rocky Mountain Foreland and the Cordilleran Thrust Belt: Geological Society of America Memoir 171, p. 75–98, https://doi.org/10.1130/MEM171-p75.

Kurz, G.A., Schmitz, M.D., Northrup, C.J., and Vallier, T.L., 2017, Isotopic compositions of intrusive rocks from the Wallowa and Olds Ferry arc terranes of northeastern Oregon and western Idaho: Implications for Cordilleran evolution, lithospheric structure, and Miocene magmatism: Lithosphere, v. 9, no. 2, p. 235–264, https://doi.org/10.1130/L550.1.

Leeman, W.P., Oldow, J.S., and Hart, W.K., 1992, Lithosphere-scale thrusting in the western U.S. Cordillera as constrained by Sr and Nd isotopic transitions in Neogene volcanic rocks: Geology, v. 20, no. 1, p. 63–66, https://doi.org/10.1130/0091-7613(1992)020<0063:LSTITW>2.3.CO;2.

Luth, S., Willingshofer, E., Sokoutis, D., and Cloetingh, S., 2010, Analogue modelling of continental collision: Influence of plate coupling on mantle lithosphere subduction, crustal deformation and surface topography: Tectonophysics, v. 484, no. 1–4, p. 87–102, https://doi.org/10.1016/j.tecto.2009.08.043.

Malone, J., Malone, J.H., Gifford, J., Craddock, J.P., Arkle, J., and Wolf, M.B., 2019, Geochronology of the southern margin of the Bighorn batholith, Wyoming: The Mountain Geologist, v. 56, no. 3, p. 267–294, https://doi.org/10.31582/rmag.mg.56.3.267.

Martinod, J., 1991, Instabilités Périodiques de la Lithosphere: University of Rennes Memoir et Documents 44, 182 p.

Martinod, J., and Davy, P., 1992, Periodic instabilities during compression or extension of the lithosphere, I. Deformation modes from an analytical perturbation model: Journal of Geophysical Research, v. 97, p. 1999–2014, https://doi.org/10.1029/91JB02715.

Maxson, J., and Tikoff, B., 1996, Hit-and-run collision model for the Laramide orogeny, western United States: Geology, v. 24, p. 968–972, https://doi.org/10.1130/0091-7613(1996)024<0968:HARCMF>2.3.CO;2.

McAdoo, D.C., and Sandwell, D.T., 1985, Folding of the oceanic lithosphere: Journal of Geophysical Research, v. 90, no. B10, p. 8563–8569, https://doi.org/10.1029/JB090iB10p08563.

McQueen, H.W.S., and Beaumont, C., 1989, Mechanical models of tilted block basins, *in* Price, R.A., ed., Origin and Evolution of Sedimentary Basins and Their Energy and Mineral Resources: American Geophysical Union Geophysical Monograph 48, p. 65–71, https://doi.org/10.1029/GM048p0065.

Mederos, S., Tikoff, B., and Bankey, V., 2005, Geometry, timing, and continuity of the Rock Springs uplift, Wyoming, and Douglas Creek Arch, Colorado: Implications for uplift mechanisms in the Rocky Mountain foreland, U.S.: Rocky Mountain Geology, v. 40, no. 2, p. 167–191, https://doi.org/10.2113/40.2.167.

Merriam, D.F., 1963, The Geologic History of Kansas: Kansas Geological Survey Bulletin 162, 275 p.

Miller, E.L., Miller, M.M., Stevens, C.H., Wright, J.E., and Madrid, R., 1992, Late Paleozoic paleogeographic and tectonic evolution of the western U.S. Cordillera, *in* Burchfiel, B.C., Lipman, P.W., and Zoback, M.L., eds., The Cordilleran Orogen: Conterminous U.S.: Boulder, Colorado, Geological Society of America, Geology of North America, v. G-3, p. 57–106, https://doi.org/10.1130/DNAG-GNA-G3.57.

Mueller, P.A., and Frost, C.D., 2006, The Wyoming Province: A distinctive Archean craton in Laurentian North America: Canadian Journal of Earth Sciences, v. 43, no. 10, p. 1391–1397, https://doi.org/10.1139/e06-075.

Oldow, J.S., Bally, A.W., Avé Lallemant, H.G., and Leeman, W.P., 1989, Phanerozoic evolution of the North American Cordillera; United States and Canada, *in* Bally, A.W., and Palmer, A.R., eds., The Geology of North America—An Overview: Boulder, Colorado, Geological Society of America, Geology of North America, v. A, p. 139–232, https://doi.org/10.1130/DNAG-GNA-A.139.

Orme, D.A., Guenthner, W.R., Laskowski, A.K., and Reiners, P.W., 2016, Long-term tectonothermal history of Laramide basement from zircon–He age–eU correlations: Earth and Planetary Science Letters, v. 453, p. 119–130, https://doi.org/10.1016/j.epsl.2016.07.046.

Palmquist, J.C., 1978, Laramide structures and basement block faulting: Two examples from the Big Horn Mountains, Wyoming, *in* Mathews, V., III, ed., Laramide Folding Associated with Basement Block Faulting in the Western United States: Geological Society of America Memoir 151, p. 125–138, https://doi.org/10.1130/MEM151-p125.

Pastor-Galán, D., Gutiérrez-Alonso, G., Zulauf, G., and Zanella, F., 2012, Analogue modeling of lithospheric-scale orocline buckling: Constraints on the evolution of the Iberian-Armorican arc: Geological Society of America Bulletin, v. 124, p. 1293–1309, https://doi.org/10.1130/B30640.1.

Paylor, E.D., II, and Yin, A., 1993, Left-slip evolution of the North Owl Creek fault system, Wyoming, during Laramide shortening, *in* Schmidt, C.J., Chase, R.B., and Erslev, E.A., eds., Laramide Basement Deformation in the Rocky Mountain Foreland of the Western United States: Geological Society of America Special Paper 280, p. 229–242 and plate, https://doi.org/10.1130/SPE280-p229.

Ramberg, H., 1963, Fluid dynamics of viscous buckling, applicable to folding of layered rocks: American Association of Petroleum Geologists Bulletin, v. 47, p. 484–505.

Ramberg, H., 1981, Gravity, Deformation and the Earth's Crust: New York, Academic Press, p. 137–194.

Ranalli, G., and Murphy, D.C., 1987, Rheological stratification of the lithosphere: Tectonophysics, v. 132, p. 281–295, https://doi.org/10.1016/0040-1951(87)90348-9.

Reiners, P.W., and Farley, K.A., 2001, Influence of crystal size on apatite (U-Th)/He thermochronology: An example from the Bighorn Mountains, Wyoming: Earth and Planetary Science Letters, v. 188, no. 3–4, p. 413–420, https://doi.org/10.1016/S0012-821X(01)00341-7.

Saleeby, J.B., 2003, Segmentation of the Laramide slab: Evidence from the southern Sierra Nevada region: Geological Society of America Bulletin, v. 115, no. 6, p. 655–668, https://doi.org/10.1130/0016-7606(2003)115<0655:SOTLSF>2.0.CO;2.

Sales, J.K., 1968, Crustal mechanics of Cordilleran foreland deformation: A regional and scale-model approach: American Association of

Petroleum Geologists Bulletin, v. 52, p. 2016–2044, https://doi.org/10.1306/5D25C549-16C1-11D7-8645000102C1865D.

Schellart, W.P., 2002, Analogue modelling of large-scale tectonic processes: An introduction: Journal of the Virtual Explorer, v. 7, p. 1–6, https://doi.org/10.3809/jvirtex.2002.00045.

Schmandt, B., Lin, F.-C., and Karlstrom, K.E., 2015, Distinct crustal isostasy trends east and west of the Rocky Mountain Front: Geophysical Research Letters, v. 42, p. 10,290–10,298, https://doi.org/10.1002/2015GL066593.

Sharry, J., Langan, R., Jovanovich, D., Jones, G., Hill, N., and Guidish, T., 1986, Enhanced imaging of the COCORP seismic line, Wind River Mountains, *in* Barazangi, M., and Brown, L., eds., Reflection Seismology: A Global Perspective: American Geophysical Union Geodynamic Monograph 13, p. 223–236, https://doi.org/10.1029/GD013p0223.

Smit, J.H.W., Cloetingh, S.A.P.L., Burov, E., Tesauro, M., Sokoutis, D., and Kaban, M.K., 2013, Interference of lithospheric folding in western Central Asia by simultaneous Indian and Arabian plate indentation: Tectonophysics, v. 602, p. 176–193, https://doi.org/10.1016/j.tecto.2012.10.032.

Smithson, S.B., Brewer, J.A., Kaufman, S., Oliver, J.E., and Hurich, C.A., 1978, Nature of the Wind River thrust, Wyoming, from COCORP deep reflection data and from gravity data: Geology, v. 6, no. 11, p. 648–652, https://doi.org/10.1130/0091-7613(1978)6<648:NOTWRT>2.0.CO;2.

Smithson, S.B., Brewer, J.A., Kaufman, S., Oliver, J.E., and Hurich, C.A., 1979, Structure of the Laramide Wind River uplift, Wyoming, from COCORP deep reflection data and from gravity data: Journal of Geophysical Research, v. 84, no. B11, p. 5955–5972, https://doi.org/10.1029/JB084iB11p05955.

Snoke, A.W., 1993, Geologic history of Wyoming within the tectonic framework of the North American Cordillera, *in* Snoke, A.W., Steidtmann, J.R., and Roberts, S.M., eds., Geology of Wyoming: Geological Survey of Wyoming Memoir 5, p. 2–56.

Sokoutis, D., and Willingshofer, E., 2011, Decoupling during continental collision and intra-plate deformation: Earth and Planetary Science Letters, v. 305, no. 3–4, p. 435–444, https://doi.org/10.1016/j.epsl.2011.03.028.

Sokoutis, D., Burg, J., Bonini, M., Corti, G., and Cloetingh, S.A.P.L., 2005, Lithospheric-scale structures from the perspective of analogue continental collision: Tectonophysics, v. 406, no. 1–2, p. 1–15, https://doi.org/10.1016/j.tecto.2005.05.025.

Stanciu, C.A., Russo, R.M., Mocanu, V.I., Bremner, P.M., Hongsresawat, S., Torpey, M.E., VanDecar, J.C., Foster, D.A., and Hole, J.A., 2016, Crustal structure beneath the Blue Mountains terranes and cratonic North America, eastern Oregon, and Idaho, from teleseismic receiver functions: Journal of Geophysical Research, v. 121, p. 5049–5067, https://doi.org/10.1002/2016JB012989.

Stanton, H.I., and Erslev, E.A., 2004, Sheep Mountain: Backlimb tightening and sequential deformation in the Bighorn Basin, Wyoming, *in* Horn, M.S., ed., Wyoming Geological Association Guidebook 2002 and Field Conference "Wyoming Basins" and 2003 Field Conference Wyoming Oil: Resources & Technology "Reversing the Decline": Casper, Wyoming, Wyoming Geological Association, p. 75–87, https://archives.datapages.com/data/wga/data/070/070001/75_wga0700075.htm.

Starostenko, V., Janik, T., Lysynchuk, D., Sroda, P., Czuba, W., Kolomiyets, K., Aleksandrowski, P., Gintov, O., Omelchenko, V., Komminaho, K., Guterch, A., Tiira, T., Gryn, D., Legostaeva, O., Thybo, H., and Tolkunov, A., 2013, Mesozoic (?) lithosphere-scale buckling of the East European craton in southern Ukraine: DOBRE-4 deep seismic profile: Geophysical Journal International, v. 195, no. 2, p. 740–766, https://doi.org/10.1093/gji/ggt292.

Stearns, D.W., 1978, Faulting and forced folding in the Rocky Mountain foreland, *in* Mathews, V., III, ed., Laramide Folding Associated with Basement Block Faulting in the Western United States: Geological Society of America Memoir 151, p. 1–37, https://doi.org/10.1130/MEM151-p1.

Steidtmann, J.R., and Middleton, L.T., 1991, Fault chronology and uplift history of the southern Wind River Range, Wyoming: Implications for Laramide and post-Laramide deformation in the Rocky Mountain foreland: Geological Society of America Bulletin, v. 103, p. 472–485, https://doi.org/10.1130/0016-7606(1991)103<0472:FCAUHO>2.3.CO;2.

Stone, D.S., 1993, Basement-involved thrust-generated folds as seismically imaged in the subsurface of the central Rocky Mountain foreland, *in* Schmidt, C.J., and Erslev, E.A., eds., Laramide Basement Deformation in the Rocky Mountain Foreland of the Western United States: Geological Society of America Special Paper 280, p. 271–318, https://doi.org/10.1130/SPE280-p271.

Stone, D.S., 2003, New interpretations of the Piney Creek thrust and associated Granite Ridge tear fault, northeastern Bighorn Mountains, Wyoming: Rocky Mountain Geology, v. 38, no. 2, p. 205–235, https://doi.org/10.2113/gsrocky.38.2.205.

Thurner, S., Margolis, R.E., Levander, A., and Niu, F., 2015, PdS receiver function evidence for crustal scale thrusting, relic subduction, and mafic underplating in the Trans-Hudson orogen and Yavapai Province: Earth and Planetary Science Letters, v. 426, p. 13–22, https://doi.org/10.1016/j.epsl.2015.06.007.

Tikoff, B., and Maxson, J., 2001, Lithospheric buckling of the Laramide foreland during Late Cretaceous and Paleogene, western United States: Rocky Mountain Geology, v. 36, no. 1, p. 13–35, https://doi.org/10.2113/gsrocky.36.1.13.

Tikoff, B., Vervoort, J.D., Hole, J.A., Russo, R., Gaschnig, R.M., and Fayon, A., 2017, EarthScope IDOR project (deformation and magmatic modification of a steep continental margin, western Idaho–eastern Oregon): Lithosphere, v. 9, no. 2, p. 151–156, https://doi.org/10.1130/L628.1.

Weil, A.B., and Yonkee, W.A., 2012, Layer-parallel shortening across the Sevier fold-thrust belt and Laramide foreland of Wyoming: Spatial and temporal evolution of a complex geodynamic system: Earth and Planetary Science Letters, v. 357–358, p. 405–420, https://doi.org/10.1016/j.epsl.2012.09.021.

Weil, A.B., Yonkee, A., and Kendall, J., 2014, Towards a better understanding of the influence of basement heterogeneities and lithospheric coupling on foreland deformation: A structural and paleomagnetic study of Laramide deformation in the southern Bighorn arch, Wyoming: Geological Society of America Bulletin, v. 126, no. 3–4, p. 415–437, https://doi.org/10.1130/B30872.1.

Whitmeyer, S.J., and Karlstrom, K.E., 2007, Tectonic model for the Proterozoic growth of North America: Geosphere, v. 3, no. 4, p. 220–259, https://doi.org/10.1130/GES00055.1.

Willingshofer, E., and Sokoutis, D., 2009, Decoupling along plate boundaries: Key variable controlling the mode of deformation and the geometry of collisional mountain belts: Geology, v. 37, no. 1, p. 39–42, https://doi.org/10.1130/G25321A.1.

Willingshofer, E., Sokoutis, D., and Burg, J.P., 2005, Lithospheric-scale analogue modelling of collision zones with a pre-existing weak zone, *in* Gapais, D., Brun, J.P., and Cobbold, P.R., eds., Deformation Mechanisms, Rheology and Tectonics: From Minerals to the Lithosphere: Geological Society, London, Special Publication 243, p. 277–294, https://doi.org/10.1144/GSL.SP.2005.243.01.18.

Worthington, L.L., Miller, K.C., Erslev, E.A., Anderson, M.L., Chamberlain, K.R., Sheehan, A.F., Yeck, W.L., Harder, S.H., and Siddoway, C.S., 2016, Crustal structure of the Bighorn Mountains region: Precambrian influence on Laramide shortening and uplift in north-central Wyoming: Tectonics, v. 35, no. 1, p. 208–236, https://doi.org/10.1002/2015TC003840.

Yeck, W.L., Sheehan, A.F., Anderson, M.L., Erslev, E.A., Miller, K.C., and Siddoway, C.S., 2014, Structure of the Bighorn Mountain region, Wyoming, from teleseismic receiver function analysis: Implications for the kinematics of Laramide shortening: Journal of Geophysical Research–Solid Earth, v. 119, no. 9, p. 7028–7042, https://doi.org/10.1002/2013JB010769.

Yonkee, A., and Weil, A.B., 2010, Reconstructing the kinematics of curved mountain belts: Internal strain patterns in the Wyoming Salient, Sevier thrust belt, U.S.A.: Geological Society of America Bulletin, v. 122, no. 1–2, p. 24–49, https://doi.org/10.1130/B26484.1.

Yonkee, A., and Weil, A.B., 2015, Tectonic evolution of the Sevier and Laramide belts within the North American Cordillera orogenic system: Earth-Science Reviews, v. 150, p. 531–593, https://doi.org/10.1016/j.earscirev.2015.08.001.

Ziegler, P.A., van Wees, J.-D., and Cloetingh, S., 1998, Mechanical controls on collision-related compressional intraplate deformation: Tectonophysics, v. 300, p. 103–129, https://doi.org/10.1016/S0040-1951(98)00236-4.

Manuscript Accepted by the Society 10 May 2021
Manuscript Published Online 18 November 2021